MAY 27 '86
214
664-F
I27.60:85-7

REC-ERC-85-7

HYDRAULIC MODEL STUDIES OF FUSE PLUG EMBANKMENTS

COMPLETED
43
ORIGINAL

December 1985
Engineering and Research Center

U. S. Department of the Interior
Bureau of Reclamation

BEST COPY AVAILABLE

7-2090 (4-81)
Bureau of Reclamation

TECHNICAL REPORT STANDARD TITLE PAGE

1. REPORT NO.	2. GOVERNMENT ACCESSION NO.	3. RECIPIENT'S CATALOG NO.
REC-ERC-85-7		

4. TITLE AND SUBTITLE	5. REPORT DATE
Hydraulic Model Studies of Fuse Plug Embankments	December 1985
	6. PERFORMING ORGANIZATION CODE: D-1532
7. AUTHOR(S): Clifford A. Pugh	8. PERFORMING ORGANIZATION REPORT NO.: REC-ERC-85-7
9. PERFORMING ORGANIZATION NAME AND ADDRESS: Bureau of Reclamation, Engineering and Research Center, Denver, CO 80225	10. WORK UNIT NO.
	11. CONTRACT OR GRANT NO.
12. SPONSORING AGENCY NAME AND ADDRESS: Same	13. TYPE OF REPORT AND PERIOD COVERED
	14. SPONSORING AGENCY CODE: DIBR

15. SUPPLEMENTARY NOTES

Microfiche and/or hard copy available at the E&R Center, Denver, CO

Editor: RNW(c)

16. ABSTRACT

Hydraulic model studies were conducted to help develop guidelines for designing fuse plugs where these structures would be appropriate for controlling reservoir outflows from large floods with long return periods. Model embankments at scales of 1:10 and 1:25 simulated prototype fuse plugs from 10 to 30 ft (3 to 9 m) high. Eight tests were conducted for a variety of embankments and flow conditions.

The erosion rates and discharge coefficients determined in this study can be used in computer flood-routing programs to aid in the design of fuse plug embankments and to assess the effects of various options.

The sand filter, embankment material, and material gradation were found to have significant effects on the rate of erosion. It was also found that the configuration of the approach channel has a significant effect on the hydraulics of the flow through the fuse plug and on the erosion rate.

17. KEY WORDS AND DOCUMENT ANALYSIS

a. DESCRIPTORS-- fuse plugs/ erosion/ flood control/ modeling/ sediment/ auxiliary spillways/ embankments/ dam breaching/ discharge coefficients/ hydraulics

b. IDENTIFIERS-- Oxbow Project, Idaho

c. COSATI Field/Group 13M COWRR: 1313 SRIM:

18. DISTRIBUTION STATEMENT	19. SECURITY CLASS (THIS REPORT)	21. NO. OF PAGES
Available from the National Technical Information Service, Operations Division, 5285 Port Royal Road, Springfield, Virginia 22161. (Microfiche and/or hard copy available from NTIS)	UNCLASSIFIED	33
	20. SECURITY CLASS (THIS PAGE) UNCLASSIFIED	22. PRICE

BEST COPY AVAILABLE

REC-ERC-85-7

HYDRAULIC MODEL STUDIES OF FUSE PLUG EMBANKMENTS

by

Clifford A. Pugh

December 1985

Hydraulics Branch
Division of Research and Laboratory Services
Engineering and Research Center
Denver, Colorado

SI METRIC

UNITED STATES DEPARTMENT OF THE INTERIOR ★ BUREAU OF RECLAMATION

BEST COPY AVAILABLE

ACKNOWLEDGMENTS

A team of engineers from the Engineering and Research Center guided the investigations, which were conducted in the hydraulics laboratory at the Engineering and Research Center, Bureau of Reclamation, Denver, Colorado. In addition to the author, the team comprised the following persons:

- Edward W. Gray, Jr., embankment dams specialist (principal investigator)
- Raymond G. Acciardi, geotechnical engineer
- Chih T. Yang, civil engineer
- Steven Higinbotham, supervisory civil engineer
- Greg G. Hammer, civil engineer

Cheryl States and B. A. Callow, civil engineering technicians, placed the model embankments. Cheryl States did the computations for model placement and composed many of the figures in the report. John C. Craig videotaped the tests and compiled and edited a video tape presentation on the research. Wayne Lambert and John Norquist were the photographers. The technical advice given by Russell A. Dodge on sediment transport was very valuable during the study.

The technical advice on modeling techniques given by Henry T. Falvey is greatly appreciated.

Edward Gray, Jr. provided valuable suggestions and review comments throughout the study.

The technical review by T. J. Rhone is greatly appreciated.

As the Nation's principal conservation agency, the Department of the Interior has responsibility for most of our nationally owned public lands and natural resources. This includes fostering the wisest use of our land and water resources, protecting our fish and wildlife, preserving the environmental and cultural values of our national parks and historical places, and providing for the enjoyment of life through outdoor recreation. The Department assesses our energy and mineral resources and works to assure that their development is in the best interests of all our people. The Department also has a major responsibility for American Indian reservation communities and for people who live in Island Territories under U.S. Administration.

The research covered by this report was funded under the Bureau of Reclamation PRESS (Program Related Engineering and Scientific Studies) allocation No. S0-3, Development of Criteria for Use in Design of Fuse Plug Embankments in Auxiliary Spillways.

The information contained in this report was developed for the Bureau of Reclamation; no warranty as to the accuracy, usefulness, or completeness is expressed or implied.

BEST COPY AVAILABLE

CONTENTS

	Page
Glossary of symbols	v
Purpose	1
Introduction	1
Conclusions	1
Literature on fuse plug erosion	2
The model	2
Description	2
Similitude	3
Hydraulic similitude	3
Sediment transport	3
Settling-velocity adjustment	4
Erosion-rate scale ratio	5
Embankment design	5
Structural similitude	6
Model measurements	6
Model results	6
Analysis	7
Effect of embankment design features	7
Core	7
Pilot channel	7
Sand filter	8
Size of embankment	8
Hydraulics of flow through the opening	8
Broad-crested weir	8
Discharge coefficients	8
Projection to prototype	9
Comparison with Oxbow field test	9
Example calculation	9
Bibliography	10

TABLES

Table		
1	Fuse plug model test data	7
2	Recommended discharge coefficients	9
3	Oxbow field-test data	9

FIGURES

Figure		Page
1	Model fuse plug embankment, test No. 7	13
2	Model operation, test No. 4	13
3	Flow-measurement weir calibration curve	14
4	Initial breach viewed through end wall, test No. 8	14
5	Forces on a sediment particle	15
6	Dimensionless unit sediment discharge curves versus dimensionless shear and grain Reynold's number	15

BEST COPY AVAILABLE

CONTENTS – Continued

Figure		Page
7	Settling velocity of sand and silt in water	16
8	Fuse plug embankment and pilot channel cross sections	17
9	Prototype gradation curves	18
10	Gradation curves, sand filter	18
11	Gradation curves, sand and gravel	19
12	Gradation curves, slope protection	19
13	Gradation curves, rockfill	20
14	Model fuse plug embankment placement	20
15	Model fuse plug embankment	21
16	Flow through the pilot channel showing the failure mode of the impervious core	21
17	Definition sketch of geometric features of model fuse plug embankment	22
18	Lateral erosion rate, test No. 1	23
19	Lateral erosion rate, test No. 2	23
20	Lateral erosion rate, test No. 3	24
21	Lateral erosion rate, test No. 4	24
22	Lateral erosion rate, test No. 5	25
23	Lateral erosion rate, test No. 6	25
24	Lateral erosion rate, test No. 7	26
25	Lateral erosion rate, test No. 8	26
26	Views of the washout process (3 sheets)	27
27	Schematic of the lateral erosion process	30
28	Broad-crested weir flow profiles, tests No. 6, 7, and 8	30
29	Weir formula discharge coefficients, test No. 7	31
30	Relative erosion rates after breach	31
31	Lateral erosion rates (after initial breach) for a fuse plug embankment with the geometric features of tests 5 and 7	32
32	Embankment design for Oxbow field test	33

BEST COPY AVAILABLE

GLOSSARY OF SYMBOLS

A	Cross-sectional area
B	Width of base of fuse plug
b	Width of base of fuse plug downstream from the core
C	Discharge coefficient
C_a	Cauchy number
C_c	Correlation coefficient
D	Reservoir water depth above fuse plug base
d	Sand grain diameter
d_{90}	Grain diameter at which 90 percent of the grains have smaller diameters
E	Modulus of elasticity
E_u	Euler number
ER	Lateral erosion rate
f	Function of
f	Friction factor
F_r	Froude number
F_c	Critical tractive force
F_w	Weight force
g	Gravitational acceleration
H	Height of fuse plug
h	Pilot channel depth
J	Crest length
k_s	Equivalent sand grain roughness
L	Distance along fuse plug crest (breach length)
l	Length
M	Structural merit number
p	Top length of pilot channel along crest
P	Pressure
Q	Water discharge
Q_s	Sediment discharge
q	Unit water discharge
q_s	Unit sediment discharge
q_s^*	Dimensionless unit sediment discharge
R	Hydraulic radius
R_e	Reynolds number
R^*	Boundary or grain Reynolds number
S	Water surface slope
S_s	Sand specific gravity
T	Impermeable core thickness
t	Clay core thickness in the model
t'	Time
u^*	Shear velocity
V	Average water velocity
w	Sediment settling velocity
W	Width of fuse plug crest in direction of flow
W_e	Weber number
γ	Specific force of water
γ_s	Specific force of sediment
θ	Angle of core with horizontal
υ	Kinematic viscosity of fluid
ρ	Density of fluid
ρ_s	Density of sediment grain
σ	Surface tension
σ_g	Standard deviation of particle sizes
τ_c	Critical shear stress
τ_o	Bed shear stress
τ^*	Dimensionless shear stress
ϕ	Friction angle

Subscript r refers to the ratio between prototype and model values.
Subscript m refers to the model.
Subscript p refers to the prototype.

BEST COPY AVAILABLE

PURPOSE

The increasing size of design floods is causing dam designers to investigate more economical methods of providing additional spillway capacity. In many cases, auxiliary spillways with fuse plug embankments can provide an economical alternative to passing all the flow through concrete structures. The Bureau of Reclamation undertook the research described in this report to help develop design guidelines to be used where a fuse plug embankment would be appropriate.

INTRODUCTION

A fuse plug is a zoned earth and rockfill embankment designed to wash out in a predictable and controlled manner when the flow capacity needed exceeds the normal capacity of the service spillway and the outlet works. A fuse plug embankment is designed to preclude use of the auxiliary spillway during minor floods, much the same as spillway gates. In many cases, auxiliary spillways with fuse plug embankments can provide an economical alternative to passing all of the flow through concrete structures.

A fuse plug is designed as a dam, stable for all conditions of reservoir operation except for a flood that will cause it to breach. The washout of a fuse plug should begin at a preselected location; general overtopping of the entire fuse plug should not occur.

The preferred method is to initiate breaching of the fuse plug with reservoir water. When the reservoir level reaches a predetermined elevation, a low spot in the embankment crest, called a pilot channel, will be overtopped.

By placing highly erodible materials in the pilot channel section, breaching will occur rapidly, and the rest of the fuse plug embankment will wash out laterally at a constant, predictable rate without overtopping. The auxiliary spillway flow will increase at a constant rate. This automatic breach feature is desirable because it reduces the possibility of mechanical or human error when operation of a flood-relief mechanism is critical. When a wide auxiliary spillway is required, it may be desirable to sectionalize the fuse plug with concrete separation walls. By using successively higher elevations for the fuse plug crests and pilot channels in each section, the washout process can be matched with successively less frequently occurring floods. The entire fuse plug would not wash out unless the full capacity of the auxiliary spillway was needed.

If the project has a gated outlet works or a service spillway, the total outflow and the reservoir elevation can be regulated as the fuse plug is washing out by controlling the flow through the gated structures.

The rate of lateral erosion as the fuse plug washes out is of primary importance. The rate of increase in downstream flow depends not only on the rate of lateral erosion, but also on the elevation of the reservoir. The rate of lateral erosion depends on the gradations and the types of materials used to construct the fuse plug, the depth of flow above the base of the fuse plug, and the geometry of the fuse plug section (crest width, angle of the upstream and downstream slopes, and configuration of the zoning).

The total discharge through an auxiliary spillway with a fuse plug embankment is controlled by the elevation of the grade sill or nonerodible foundation beneath the fuse plug, by the width of the spillway channel, by the depth of water above the grade sill or foundation, and by the width of the grade sill in the direction of flow.

The rates of lateral erosion and coefficients of discharge obtained from the research described in this report can be used in a computer flood-routing program to predict the downstream flows and reservoir water surface elevations. The effects of varying the rate of lateral erosion and the elevation of the pilot channel on the reservoir elevation and on the auxiliary spillway discharge can also be determined.

The auxiliary spillway should be designed according to standard practice. The flow velocities must be sufficient for the water to carry the eroded fuse plug material downstream to avoid clogging of the return channel to the natural stream course. If excessive sediment deposition is anticipated, a site-specific model study may be required to design the return channel. If the approach channel to the fuse plug is relatively shallow and long, losses may limit the discharge and further study may be required.

CONCLUSIONS

- A properly designed fuse plug embankment will wash out in an orderly and predictable manner when additional flow capacity is needed to pass a large flood through a reservoir. The fuse plug will preclude the use of the auxiliary spillway during small floods.

- The lateral erosion rate (after the initial breach) is primarily a function of the erosion rate of the embankment material and not a function of the strength of the impermeable core.

- The erosion rates and discharge coefficients determined in this study can be used in flood-routing

BEST COPY AVAILABLE

computer programs to help design fuse plug embankments.

- Ratios of depth of water to embankment height and depth of water to weir width have significant effects on erosion rates.
- The sand filter, embankment material, and gradation have significant effects on erosion rates.
- A model design method is described that compensates for the fact that the Reynolds number is normally too low to properly simulate sediment transport in a Froude scale hydraulic model. This method uses settling velocity adjustments and dimensionless unit sediment discharges to adjust the model grain sizes and/or the model sediment density.

LITERATURE ON FUSE PLUG EROSION

Fuse plug embankments have been designed and constructed for mine tailing dams, for levees, and for controlling the flow in auxiliary spillways. However, there has not been a documented case of a fuse plug controlled spillway actually operating. Most of the information in the literature is associated with studies conducted in 1959, to design a fuse plug-controlled spillway for the Oxbow Project, on the Snake River between Idaho and Oregon [1, 2, 3].*

The Oxbow Project has two spillways, each with a design flow capacity of 150,000 ft^3/s (4250 m^3/s), which is on the order of the 100-year flood. The total discharge capacity of 300,000 ft^3/s (8500 m^3/s) corresponds to the inflow design flood. The original design required three radial gates to control each spillway. Later, the Idaho spillway, on the right abutment, was changed to fuse plug control [3]. The studies conducted to confirm the design assumptions included 1:20 and 1:40 scale model tests in the laboratory and a 1:2 scale field test at the damsite.

Another study of erosion mechanics and washout time rates of erodible control embankments was made using hydraulic models at the University of Windsor, in 1977 [4]. This study analyzed theoretical equations and compared calculations with model results.

THE MODEL

Description

The model was designed to simulate typical prototype fuse plugs from 10 to 30 ft (3 to 9 m) high. The model embankments were from 0.5 to 1.25 ft (0.15 to 0.38 m) high and 8.8 ft (2.7 m) long, at scales of 1:10 and 1:25, (fig. 1). The model size was based on the maximum flow available in the laboratory. A flow of 21.5 ft^3/s (0.61 m^3/s) was made possible by using two pumps operated in parallel.

The overall model was 46 ft (14 m) long by 26 ft (8 m) wide. Flow entered the model through two 1-ft (0.3-m) pipes and passed through a rock baffle into a 17-ft (7.6-m) by 5-ft (1.5-m) deep headbox (fig. 2). The headbox simulated a reservoir in a prototype structure. The water surface level in the headbox was controlled by a 25-ft (7.6-m) long adjustable-height weir along one side. Water flowing over the adjustable weir plunged into a side channel, then it passed through a flow-measurement weir. The flow-measurement weir, a combination-type weir, was calibrated for flow versus water surface elevation in the side channel. The lower 1 ft (0.31 m) of the weir had a 90° V-notch. Above the V-notch were 2-ft (0.61-m) extensions on each side at a 15° angle with horizontal. Above these 15° extensions were 1.5-ft (0.46-m) long vertical sides. The calibration curve for the measurement weir is shown on figure 3. The calibration was done in three parts corresponding to the three different sections of the weir. During each test, the calibration curve shown on figure 3 was used to compute the discharge through the measurement weir. Water surface elevations were monitored with capacitance-type water surface probes. The data were recorded on disc with a microcomputer.

The fuse plug embankment platform was located at the end of the headbox, 2.5-ft (0.76 m) above the headbox floor. One end wall of the platform was constructed from transparent plastic to observe the initial breach and lateral erosion process (fig. 4). A sloping platform downstream from the horizontal fuse plug platform led to a tailbox where the sediment was deposited before the water returned to the laboratory supply reservoir. A typical test used the following procedure:

1. With the adjustable control weir at a low level, the valves controlling the two inlet pipes were opened; the entire flow of 21.5 ft^3/s (0.61 m^3/s) entered the headbox, passed over the control weir and through the measurement weir.

2. The test was started by raising the reservoir water surface with the control weir to a predetermined level where water began flowing through the pilot channel.

3. As the fuse plug embankment washed away, more water passed through the breach. The water surface was kept at a constant level by gradually raising the control weir.

BEST COPY AVAILABLE

4. The flow through the measurement weir, the level of the water surface in the reservoir, and the time were recorded continually. Each test was videotaped and photographed.

5. Flows through the breach were computed by subtracting the measurement weir readings from the total (initial) flow.

Similitude

Hydraulic model studies are used because of the large number of variables involved in hydraulics and because of the differences in boundary configurations. The physical behavior of a model simulates, in a known manner, the physical behavior of the prototype.

There are several types of similarity. Geometric similarity exists when the ratios of all homologous dimensions between the model and the prototype are the same. The geometric scale ratio, or length ratio, is denoted by $L_r = L_m/L_p$, where the subscripts m and p refer to the model and the prototype, respectively.

Kinematic similarity, or similarity of motion, implies that the ratios of velocities and accelerations between the model and prototype are equal.

Dynamic similarity requires that the ratios of homologous forces between the model and prototype be the same. In the study of hydraulic phenomena, the primary forces that influence the flow are the forces due to gravity, viscosity, pressure, surface tension, and elasticity. The inertial force is the vector sum of all the forces [5]. The following dimensionless numbers relate inertial force to each of the forces listed above.

Froude number (inertia/gravity), $F_r = \frac{V}{Lg}$ (1)

Reynolds number (inertia/viscosity), $R_e = \frac{VL}{\upsilon}$ (2)

Euler number (inertia/pressure), $E_u = \frac{\rho V^2}{\Delta p}$ (3)

Weber number (inertia/surface tension), $W_e = \frac{\rho L V^2}{\sigma}$ (4)

Cauchy number (inertia/elasticity), $C_a = \frac{\rho V^2}{E}$ (5)

It is apparent that a model fluid cannot simulate all of these properties concurrently. However, in most cases several of the forces will be absent or negligible in the model. Therefore, a model can usually simulate the critical prototype forces for a certain type of flow.

Hydraulic similitude. – The flow of water through a fuse plug is primarily determined by gravity and inertia forces; the other forces may be neglected. The ratios between the model and prototype are determined from the Froude law (equation 1). The scale relations according to the Froude law are as follows:

Ratio	Scale relation (model/prototype)
Length	$= L_r$ (geometric ratio)
Area	$= L_r^2$
Volume	$= L_r^3$
Time	$= t_r' = \frac{L_r^{1/2}}{g_r} = L_r^{1/2}$ (for $g_r = 1$)
Velocity	$= V_r = L_r/t_r' = L_r^{1/2}$
Discharge	$= Q = L_r^{5/2}$

Sediment transport. – Vanoni [6] discussed the important variables involved in the present knowledge of sediment transport in a section on "Fundamentals of Sediment Transport." He reduced the sediment discharge rate, Q_s, to the following relationship. These symbols are defined in the glossary.

$$Q_s = f(Q, R, d, \upsilon, \rho, \rho_s, \sigma_g, w, g) \quad (6)$$

Models involving erosion of noncohesive bed material must simulate tractive stress (τ_o) because the tractive stress causes the drag force required to overcome the forces holding a particle in place (fig. 5).

The tractive stress on a particle fluctuates because of the turbulence. The drag force and turbulence are a function of the Reynolds number (equation 2). Therefore, a model operated according to Froude scaling does not necessarily simulate the tractive forces and sediment erosion accurately. In some models the sediment sizes must be adjusted to compensate for a Reynolds number that is too low.

Shields developed a diagram relating dimensionless shear stress (τ^*) to a boundary or grain Reynolds number (R^*). Shields used this diagram to define critical shear stress (τ_c) (the stress required for incipient motion of sediment). This concept has been expanded by others to include dimensionless unit sediment discharge.

$$q_s^* = \frac{q_s}{u^* d} \quad (7)$$

BEST COPY AVAILABLE

Vanoni [6] used Taylor's data to show that dimensionless unit sediment discharge at low transport levels falls very close to the Shields curve for incipient motion (figure 6). To properly simulate sediment transport, the dimensionless unit sediment discharge rate (q_s^*) must be the same in the model and the prototype.

For a model with a grain Reynolds number (R^*) greater than 5 and less than 100, the unit sediment discharge rate for the model would be higher than that for the prototype (if the model sand grains are sized according to geometric scaling). Because the dimensionless shear stress (τ^*) is about the same in the model and the prototype where:

$$\text{Grain Reynolds number, } R^* = \frac{u^* d}{\upsilon} \tag{8}$$

and

$$\text{Dimensionless shear stress, } \tau^* = \frac{\tau_o}{(\gamma_s - \gamma)d} \tag{9}$$

it can be shown that dimensionless shear stress is a form of the Froude number and the density ratio of the sediment and of the water.

$$\text{The shear velocity, } u^* = \sqrt{\frac{\tau_o}{\rho}} \tag{10}$$

$$\text{therefore, } \tau_o = \rho u^{*2} \tag{11}$$

$$\text{and the unit force, } \gamma = \rho g \tag{12}$$

Substituting equation (12) into equation (11):

$$\tau_o = \gamma u^{*2}/g \tag{13}$$

Substituting equation (13) into equation (9):

$$\tau^* = \left(\frac{u^{*2}}{gd}\right)\left(\frac{\gamma}{\gamma_s - \gamma}\right) \tag{14}$$

The first term in equation (14) is in the form of a Froude number, the second term is the ratio of the densities of the water and the sediment, when gravity is factored out.

It is sometimes more convenient to compute τ^* by using a form of equation (9) relating τ^* to the Darcy-Weisbach friction factor (f). Rouse [7] has shown that the shear velocity,

$$u^* = \sqrt{gRS} = \sqrt{\frac{\tau_o}{\rho}} = V\sqrt{\frac{f}{8}} \tag{15}$$

Substituting equation (15) into equation (14),

$$\tau^* = \left(\frac{V^2 f}{8gd}\right)\left(\frac{\gamma}{\gamma_s - \gamma}\right) \tag{16}$$

To determine f in an open channel, the Reynolds number (R_e) is computed according to the following equation.

$$R_e = 4RV/\upsilon \tag{17}$$

where R = the hydraulic radius. The relative roughness (needed to determine f) is defined as:

$$\text{relative roughness} = K_s/4R \tag{18}$$

where K_s = rugosity.

Kamphius [8] found that

$$K_s = 2\ d_{90} \tag{19}$$

where d_{90} = the particle diameter at which 90 percent of the grains are smaller in diameter.

The hydraulic radius can be taken as the flow depth, if the channel is relatively wide.

If a model is scaled geometrically according to Froude scaling ($\tau_m^* = \tau_p^*$), the model unit sediment discharge rate (q_s^*) will be too great in the range $5 < R^* < 100$. Therefore, the model should be adjusted to properly simulate sediment transport in this range. A diagram of settling velocity (w) of sand and silt particles in water (fig. 7) illustrates that small particles (< 1 mm in diameter) settle at slower velocities as the particles become smaller. For particle diameters larger than (1 mm), the settling velocity is a function of the particle diameter (d) to the 1/2 power. This is consistent with Froude scaling for velocity, $V_r = L_r^{1/2}$ (see the previous section on hydraulic similitude).

Settling-velocity adjustment. – By increasing the size of a model sediment grain, the settling velocity can be corrected to the proper value for Froude scaling. According to geometric scaling, a 1:10 scale model of prototype sand 2.0 mm in diameter would use sand 0.2 mm in diameter. However, the settling velocity would then be about 0.066 ft/s (0.02 m/s) (see fig. 7), when it should be 0.161 ft/s (0.049 m/s), according to Froude scaling. If the model particle size is increased from 0.2 to 0.4 mm, the settling velocity is corrected to 0.161 ft/s (0.049 m/s), the proper value for Froude scaling.

The effect of settling velocity adjustment on the dimensionless sediment discharge rate (q_s^*) is shown on figure 6. Note that the model values of τ^* before the settling velocity adjustment are about the same

BEST COPY AVAILABLE

as prototype values they simulate. Tests No. 1-5 simulate the 25-ft (7.6 m) high prototype embankment, and tests No. 6, 7, and 8 simulate the 12.5-ft (3.8 m) high prototype embankment. However, the value of q_s^* must be the same in the model and prototype to properly scale the time rate of sediment transport. When the model grain sizes are adjusted for settling velocity (as described above) the value of τ^* decreases, while the value of R^* increases. This brings the model value of q_s^* much closer to the projected prototype value of q_s^* (upper pair of curved lines on figure 6). In this study, the model grain sizes were computed using this method of settling-velocity adjustment to account for the low grain Reynolds number. This method applies to noncohesive materials in the model and in the prototype, and must be checked for each grain size and each model flow condition. If model Reynolds number (R^*) is less than 5, a lighter sediment specific force (γ_s) could be substituted to match q_s^*. If R^* is greater than 100, no adjustment is necessary.

Erosion-rate scale ratio. – After the settling-velocity is adjusted as described above, the erosion rate scales according to the Froude law. Velocities scale according to $L_r^{1/2}$; therefore, lateral erosion rate is:

$$(ER)_r = L_r^{1/2} \qquad (20)$$

The small-scale model tests conducted for the Oxbow Project used prototype diameter uniform-sized materials in the model. For these materials, Tinney and Hsu [1] concluded that the erosion rate ratio would be, $(ER)_r = L_r^{1/3}$. Chee [4] derived the following equation for the erosion-rate scale ratio,

$$(ER)_r = L_r^{0.375} (S_s - 1)_r^2 d_r^{0.13} \qquad (21)$$

where S_s is the sand specific gravity. If $(S_s - 1)_r = 1$ (the same density sand in the model and the prototype) and $d_r = L_r$ (geometric scaling), then $(ER)_r = L_r^{0.505}$. This is very close to the Froude scaling ratio obtained in this analysis, $(ER)_r = L_r^{1/2}$. However, Chee's method does not account for a low grain Reynolds numbers in the model.

For $(S_s - 1)_r = 1$ and $d_r = 1$ (prototype-sized grains in the model), the erosion-rate ratio derived by Chee is approximately that derived by Tinney and Hsu, $L_r^{0.375}$ versus $L_r^{1/3}$.

Embankment design. – The fuse plug embankment was designed with the same zones found in most zoned-material rockfill dams. The arrangement of these zones is shown on figure 8. The main difference between a fuse plug embankment and a typical rockfill or earthfill dam is the arrangement of the impervious core. The core of a fuse plug embankment is inclined so that when the downstream material is washed away, pieces of the core break off from bending under its own weight and under the water load. The core material is normally silt or clay. The sand filter prevents piping through cracks that develop in the core and keeps windblown silt and clay from infiltrating the downstream embankment material. The compacted sand and gravel and compacted rockfill are designed to be noncohesive and easily erodible once the washout process begins. The prototype gradation curves for each zone are shown on figure 9. A range of acceptable sizes are shown with the gradation simulated in the model study indicated by a dashed line.

The model and prototype gradation curves for each zone are shown on figures 10 through 13. These model gradation curves were determined by making settling-velocity adjustments to the grain sizes determined by geometric scaling. The adjustments in grain sizes do not significantly affect the shapes of the model gradation curves.

The pilot channel section was designed to wash out quickly when the water flowed through the pilot channel. A slightly larger rockfill material with fewer sand sizes was used in this section to ensure a rapid break. The prototype pilot channel was designed to be 3 ft (0.9 m) deep: 1 ft (0.3 m) of water depth and 2 ft (0.6 m) of freeboard. This depth of water was determined to be adequate to initiate a breach during the Oxbow study. The width of the pilot channel was investigated in this model study. The side slopes of the pilot channel were set at 1:1; however, this value could be varied in the prototype. The gradation and compaction of the noncohesive materials are important factors in determining the erosion rate. As the materials are compacted, more tractive force is required to remove the grains because there are more grains per unit volume and more contact and interlocking between them. A well-graded mixture of grain sizes requires more tractive force to erode than uniform-sized material requires. Smaller particles fill the voids between larger particles, making the mixture more dense and creating more contact between the particles.

For the reasons cited above, great care was taken in placing the model fuse plug embankments. Relative density tests were conducted on the model materials before they were placed. (See gradation curves on figs. 10, 11, and 13.)

The method consisted of placing a predetermined weight of material in a given volume to obtain 70 percent relative density. The proper proportion of

* Numbers in brackets refers to bibliography.

BEST COPY AVAILABLE

each of the material sizes was mixed to obtain the desired gradation. A known weight of the mixture was then placed in a known volume in the model (fig. 14). The volume in the model was controlled by using wooden forms 1½ to 2 in (38 to 51 mm) thick. The main embankment downstream from the core (zones 3 and 6 on fig. 8) was placed in layers using this method. The compaction was obtained by using a compressed-air powered vibrator and tamping tools. When the placement of this zone was complete, the forms were removed and the corners were trimmed to the correct slope. The sand filter, core, embankment upstream from the core, slope protection, and gravel surfacing were then installed using templates and tamping tools. A completed model fuse plug embankment is shown on figure 15.

Structural similitude. – The impervious core was not simulated as part of the hydraulic modeling because the cohesive clay portion does not fail as a result of sediment erosion. The core is designed to break off in pieces from the weight of the water and embankment material above it, as the non-cohesive material downstream washes away. Figure 16 is a schematic diagram illustrating the failure mode of the materials in the pilot channel. The core fails in a similar manner during the lateral erosion process, as the material on the face of the embankment downstream from the core is washed away.

The structural behavior of the core material was simulated qualitatively, because the prototype core material strength will vary a great deal. A structural analysis of the prototype core as a cantilevered slab indicates that only about 2.9 ft (0.88 m) of core would overhang horizontally before it would break [assuming a high tensile strength in the core of 1000 lb/in^2 (6895 KPa)].

The structural behavior of the core material is governed by gravity and elasticity forces. The structural merit number (M) is the dimensionless ratio of gravity forces to elasticity forces.

$$M = \frac{\gamma L}{E} \tag{22}$$

where E = modulus of elasticity of the core.

For structural similitude:

$$\left(\frac{\gamma L}{E}\right)_m = \left(\frac{\gamma L}{E}\right)_p \tag{23}$$

If $\gamma_m = \gamma_p$, then

$$\frac{E_m}{E_p} = \frac{L_m}{L_p} = L_r \tag{24}$$

The ratio of the moduli of elasticity must equal the model scale ratio. However, it is difficult to find a model core material that has a modulus of elasticity low enough to satisfy this ratio and maintain a seal. Therefore, a mixture of 10 percent clay and 90 percent sand with a modulus of elasticity approximately equal to that of the prototype was used.

Because the model modulus of elasticity (E_m) was too large, the core thickness had to be reduced to compensate. A clay core reduced in thickness (⅓ of geometric scaling) was used in most of the tests. This thickness resulted from computing the correct moment of inertia in the model to compensate for the modulus of elasticity being too large in the model. The remainder of the core thickness was built with sand sprayed with a stabilizing agent (which added no strength).

Model Measurements

During each test several measurements were made to document the washout.

1. Bypass flow was recorded at 3-second intervals. The measured weir flow was subtracted from the total inflow to obtain the flow through the breach.

2. The reservoir level was recorded continuously.

3. Flags were placed on the top of the embankment at 1-ft intervals, and a grid pattern was painted on the downstream face of the embankment. The lateral erosion rates (ER) were recorded by noting the time that the erosion reached each flag. These rates were checked by viewing the video tape.

4. Each test was filmed using video tape cameras, still photographs, and slides. One video camera was located downstream from the embankment, and the other filmed the washout through the acrylic plastic end wall.

5. The discharge, reservoir level, and the time were recorded on a floppy disk with the aid of a microcomputer.

Model Results

The erosion process and lateral erosion rate are partially dependent on the geometric configuration of the embankment. Figure 17 shows the configuration of the model embankments tested and defines the symbols. Table 1 lists the values of each of the pertinent features for each test. These values are listed as dimensionless ratios of the fuse plug height (H).

BEST COPY AVAILABLE

The rate of erosion was consistent throughout the test for any one model configuration and flow condition (see figs. 18 through 25). The erosion rate varied as the model configuration or flow condition was changed. The first constant in the regression equations, shown on each graph, is the lateral erosion rate.

Before each test the reservoir level was held constant at a level below the pilot channel invert, with a long adjustable weir. The test was begun by raising the water surface to a level equivalent to a 1 ft (0.3 m) water depth in the prototype pilot channel. The material downstream from the core eroded down to the base of the fuse plug. When the support was removed from beneath, a piece of the core broke off. This process recurred until the material in the pilot channel was completely washed away. Figure 26 is a series of photographs illustrating the erosion process.

After the initial breach, the embankment eroded laterally. The flow eroded the face of the embankment downstream from the core in a steady, continuous manner. As the noncohesive material washed away and the support was removed, pieces of the core broke off. Figure 27 is a schematic diagram illustrating how water flowed around the core and eroded the downstream embankment.

ANALYSIS

An analysis was made of the model results to determine the effect of the pertinent geometric and flow parameters.

Effect of Embankment Design Features

Core. – The role and the effect of the impervious core were analyzed in the model study. A previous section on "Structural Similitude" discusses the structural modeling of the core. A clay core one-third the thickness indicated by geometric scaling was used during most tests.

To assess the effect of the core thickness on the lateral erosion process, one test was conducted with a clay core thickness indicated by geometric similitude (test No. 2). This thickness was about three times greater than that required for structural similitude. The strength was about 25 times greater than required. During this test the initial breach proceeded about the same as in the other tests up to the point of the first core break, which did not occur naturally. The first break was assisted by manually breaking the clay, after which the washout process proceeded much the same as in the other tests. The lateral erosion rate was 1.52 ft/min (0.463 m/min), which was only 2 percent less than that in an essentially identical test with a thinner clay core [test No. 4, ER = 1.55 ft/min (0.472 m/min)]. During the lateral erosion process in test No. 2, the noncohesive material downstream from the core eroded at a constant rate and the core broke off in bigger pieces than it did in the other tests.

Test No. 2 indicates that the lateral erosion rate (after the initial breach) is primarily a function of the erosion rate of the noncohesive material downstream from the core and not a function of the core strength.

During test No. 3 the core was installed at an angle 30° above horizontal (table 1). The material downstream from the core was shielded more by the core, and the initial breach took longer. The lateral erosion rate was about the same. It was decided to use a core angle of 45° for the remaining tests to prevent excessive shielding of the downstream materials.

Pilot channel. – Various widths and positions of the pilot channel were tested. The location of the pilot channel did not have a noticeable effect on the lateral erosion rate. The erosion rate for test No. 4, with the pilot channel located near the center of the embankment, was the same in both directions, and about the same as the erosion rate of a similar test with the pilot channel close to one end of the embankment.

Table 1. – Fuse plug model test data.

Test No.	H, ft	Scale	W/H	B/H	b/H	θ deg	T/H	t/H	L/H	p/H	h/H	Sand filter	D/J	D/H	ER, ft/min
1	1.0	1:25	0.4	4.4	3.1	45	0.12	0.04	0.0	0.24	0.12	Yes	0.21	0.92	1.74
2	1.0	1:25	.4	4.4	3.1	45	.12	.12	.12	.36	.12	No	.21	.92	1.52
3	1.0	1:25	.4	4.4	4.0	30	.12	.04	.32	.48	.12	No	.21	.92	1.53
4	1.0	1:25	.4	4.4	3.1	45	.12	.04	3.24	.48	.12	No	.21	.92	1.55
5	1.0	1:25	.8	4.8	3.4	45	.12	.04	0.45	.74	.12	Yes	.15	.92	1.60
6	0.5	1:25	.8	4.8	3.4	45	.12	.04	.91	1.48	.24	Yes	.07	.84	0.68
7	1.25	1:10	.8	4.8	3.4	45	.12	.04	.51	0.88	.24	Yes	.17	.84	1.66
													*.15	*.73	*1.43
8	1.25	1:10	.8	4.8	3.4	45	.12	.04	1.60	3.20	.24	Yes	*.12	*.60	*0.63

Refer to figure 17 for definitions of the symbols.
1 ft = 0.3048 m
* The upstream water level (D) was lowered.

BEST COPY AVAILABLE

The width of the pilot channel controls the amount of water passing through to initiate the breach. Qualitative observations of the model tests indicate that the pilot channel width (p) should be about ½ of the fuse plug height ($p/H \geq 0.5$) to ensure that adequate breaching flow passes through the pilot channel.

Sand filter. – Tests were run with and without the sand filter surrounding the main embankment downstream from the core. (See fig. 8 for embankment zoning.) It was found that the sand filter has a significant effect on both the initial breach and the lateral erosion. Without the filter, the water flowing through the pilot channel infiltrates the downstream noncohesive material and partially saturates this zone, thus prolonging the breaching process. The lateral erosion rate is also significantly slower when the downstream sand filter is removed. Test No. 1 and test No. 4 have identical embankment designs, with the exception of the sand filter. The erosion rate for test No. 4, without the sand filter, is about 11 percent slower. The volume of the compacted sand and gravel zone is greater without the sand filter because the sand and gravel also occupy the sand-filter zone. The compacted sand and gravel particles require more tractive force to move because these particles are larger and their sizes vary more than those in the sand filter material. This causes more particle interlocking.

Size of embankment. – The relative size of the embankment was investigated in test No. 5. The width of the fuse plug crest was doubled, increasing the area of the eroding face of the embankment. The erosion rate for test No. 5 was about 8 percent less than that for test No. 1. This is about the same percentage as the increase in the area of the cross section of the downstream compacted sand and gravel zone.

Hydraulics of Flow Through the Opening

Broad-crested weir. – Flow through the opening is similar to flow over a broad-crested weir. The broad-crested weir flow depends on the depth of water above the crest (D) and the length of the crest (J). In the range of $0.08 < D/J < 0.5$ [9], flow over a horizontal crest is in the broad-crested weir flow range. Figure 28 shows broad-crested weir flow profiles for tests No. 6, 7, and 8. For broad-crested weir flow, the top surface and flow streamlines become parallel with the horizontal crest. The flow discharge is controlled by the critical flow depth near the end of the crest [10]. If $D/J < 0.08$ the flow depth is controlled by friction on the crest.

Discharge coefficients. – The following equation expresses discharge over a weir as a function of water depth.

$$Q = CLH^{3/2} \tag{25}$$

For critical depth, $d_c = (2/3)H$, and using the Froude number at critical depth:

$$F_r = 1 = \frac{V}{\sqrt{gd_c}} \tag{26}$$

Equation 26 can be expressed as:

$$q = g^{1/2}(2/3)^{3/2}H^{3/2}$$

or

$$q = 3.09\ H^{3/2} \tag{27}$$

where the unit discharge, $q = Vd_c$

The coefficient (C) in equation (25) is 3.09 $ft^{1/2}/s$ (1.70 $m^{1/2}/s$)

For a broad-crested weir, the critical depth point is actually slightly upstream from the downstream end of the crest, and the losses reduce the theoretical value of C slightly. Empirical data [9] indicate that in the broad-crested weir range $0.08 \leq D/J \leq 0.5$, the theoretical discharge coefficient is reduced by a factor of 0.848. Therefore, equation 25 would be:

$$Q = 0.848\ (3.09)\ LH^{3/2}$$

or

$$Q = 2.62\ LH^{3/2} \tag{28}$$

Discharge coefficients measured during test No. 7 are shown on figure 29. These coefficients were computed from the discharge and water depth measurements made during the test. The discharge coefficients increase to a maximum value of 2.78 $ft^{1/2}/s$ (1.53 $m^{1/2}/s$) for a breach length (L) of 4 to 6 ft (1.2 to 1.8 m). The coefficient drops slightly, to $C = 2.62$ $ft^{1/2}/s$ (1.44 $m^{1/2}/s$) when the embankment is completely washed away. This value matches the empirical value for a broad-crested weir (equation 28). The higher discharge coefficient during the washout can be attributed to a longer effective weir length caused by the flow coming around the face of the embankment (fig. 27). During test No. 6 ($D/J < 0.08$) the flow on the crest was controlled by friction. In test No. 4 with erosion in both directions the relative weir length was increased during washout by the flow coming around the face of the embankment on each side (fig. 27). The discharge coefficient was 3.1 $ft^{1/2}/s$ (1.71 $m^{1/2}/s$) during washout. Table 2 summarizes the recommended discharge coefficients for flood-routing studies.

These discharge coefficients can be used in a computer flood-routing program after the initial breaching has occurred. The lateral erosion rate is a function

BEST COPY AVAILABLE

Table 2. – Recommended discharge coefficients (equation 25).

	C	
	$m^{1/2}/s$	$ft^{1/2}/s$
In the broad-crested weir range ($0.08 < D/J < 0.5$)		
During washout in one direction	1.51	2.75
During washout in both directions	1.71	3.10
After washout is complete	1.44	2.62

of the flow depth to crest length ratio (D/J) and the depth to fuse plug height ratio (D/H). Tests No. 6 and 7 have the same D/H ratio (0.84), but different D/J ratios (fig. 28). The result is a different erosion process. For $(D/J) > 0.12$, the flow surface was still drawing down as it reached the embankment. This caused a longitudinal vortex along the face of the downstream compacted sand and gravel that accelerated the erosion rate. For $D/J < 0.12$, the flow was parallel to the crest as it reached the embankment. The erosion was similar to streambank erosion with no vortex caused by drawdown to aid the erosion process.

Relative erosion rates are shown as a function of water depth (D) and crest length on figure 30. This figure illustrates that the relative erosion rate is a power function of the water depth ratio for $D/J < 0.12$. For $D/J > 0.12$, the erosion rate is much faster. The data on this graph are scaled to the same size embankment by the erosion-rate scale relationship according to Froude scaling.

This analysis illustrates that the length of weir (J) has a major effect on the erosion process.

Projection to Prototype

The results from this study can be used to predict the behavior of a prototype fuse plug embankment designed as described in this report. The discharge coefficients discussed in the previous sections can be used to predict the flow through a given size opening.

The lateral erosion rate (after the initial breach) for a given embankment design and flow depth can be predicted from the model tests. Figure 31 shows the erosion rates for an embankment with the geometric configuration given in table 1 for tests No. 5 and 7. The flow depth was determined by the pilot channel design, with 2 ft (0.6 m) of freeboard and 1 ft (0.3 m) of water depth, regardless of the embankment height. Equation 29 is an empirical equation that can be used to estimate erosion rates for embankments of this configuration that are from 10 to 30 ft (3 to 9 m) high.

$$ER = 13.2\ H + 150 \qquad (29)$$

If the configuration of the embankment or the flow condition is changed, the erosion rate given by equation 29 would be changed accordingly. For example, if the cross-sectional area of the downstream compacted sand and gravel section is decreased by 10 percent, the erosion rate predicted by equation 29 should be increased by 10 percent. If the water depth (D) or crest length (J) are different from those on figure 31, the erosion rate would be adjusted using figure 30. This adjustment would also be used if the reservoir level changes during the washout process.

Comparison with Oxbow Field Test

The only data available on a prototype-size fuse plug in operation are for a field test performed as part of the design of a fuse plug control for an auxiliary spillway on the Oxbow Project on the Snake River in Idaho. The ½-scale field test of a 27 ft (8.2 m) prototype embankment showed the same pilot channel breach and lateral erosion process indicated by this model study. The following are the geometric and flow parameters for the Oxbow field test (as defined on fig. 17).

The Oxbow embankment design [1] is shown on figure 32. The gradation curve for the Oxbow zone 4 (concrete aggregate) was similar to that of the prototype zone 3 (compacted sand and gravel) simulated in this study (fig. 11).

Although the embankment designed for the Oxbow field test was slightly different from the embankments tested in this model study, the erosion rate was close to the erosion rate predicted by equation 29 (fig. 31).

During the later stages of the Oxbow field test, the entire embankment downstream from the sand filter was zone 3 (well-graded) material. The erosion rate reduced from 336 to 72 ft/h (102 to 22 m/hr), demonstrating the importance of material gradation. This drastic reduction in erosion rate was caused by the cohesion of the well-graded zone 3 material.

Table 3. – Oxbow field test data (1 ft = 0.3048 m).

H, ft	W/H	B/H	b/H	θ	T/H	L/H	p/H	h/H	Sand filter	D/H	ER, (ft/min)
13.5	0.37	4.12	2.59	45°	0.11	0.37	0.81	0.15	Yes	0.93	5.6

Example Calculation

Find the erosion rate and discharge through a fuse plug with the following dimensions:

H = 17.5 ft (5.33 m) θ = 45°

W = 10.0 ft (3.05 m) h = 3.00 ft (0.91 m)

p = 13.0 ft (4.00 m)

BEST COPY AVAILABLE

The nonerodible base for the fuse plug is cut into rock in the abutment of the dam. The pilot channel is at one end of the fuse plug and the fuse plug embankment is 2000 ft (610 m) long. The fuse plug base is an average of 200 ft (61 m) wide in the direction of the flow. The upstream and downstream slopes of the embankment are 2:1.

The solution is:

$$W/H = 0.57 \text{ and } h/H = 0.14$$

If it is assumed that the downstream edge of the core intersects the top of the fuse plug at the center (fig. 8), then

$$b/H = 3.29 \text{ (from geometry)}$$

If the pilot channel breaches when the water is 1 ft (0.3 m) deep, $D = H - h + 1$ ft = 15.5 ft (4.72 m), and

$$D/H = 0.89,\ D/J = 0.08$$

The erosion rate (*ER*), is then computed for the reference case (fig. 31, tests 5 and 7) using equation 29:

$$ER = 13.2\ H + 150 = 381 \text{ ft/h} \quad (116 \text{ m/h})$$

Because the reference embankment is larger than that in the example ($W/H = 0.8$ and $b/H = 3.4$), an adjustment is needed. The area of the cross section downstream from the core for the example is about 5 percent less than that for the reference embankment (from the geometry of the cross section). Therefore, the lateral erosion rate should be increased from the computed value, because there is less material to erode.

$$\text{Adjusted } ER = 1.05 \times \text{reference } ER = 1.05 \times 381 = 400 \text{ ft/h} \quad (121 \text{ m/h})$$

Water depth to fuse plug height ratio (D/H) is the same in the example and in the reference ($D/H = 0.89$). However, the water depth to crest length ratio (D/J) is much less in the example (0.08 vs. 0.17).

The relatively long approach channel has a significant effect on the erosion rate (fig. 30). To make the adjustment for a long approach channel, the relative erosion rate for $D/J < 0.12$ is divided by the relative erosion rate for $D/J > 0.12$. This ratio is multiplied by the calculated erosion rate for the example (fig. 30):

$$\frac{\text{Relative erosion rate } (D/J < 0.12,\ D/H = 0.89)}{\text{Relative erosion rate } (D/J > 0.12,\ D/H = 0.89)} = \frac{0.62}{0.89} = 0.70$$

$$ER \text{ reduction ratio} = 0.70$$

$$\text{Adjusted } ER = 0.70\ (400) = 280 \text{ ft/h } (85.3 \text{ m/h})$$

If the reservoir level remains about the same during the washout, the embankment would wash out at a constant rate in 7.1 h [2000 ft/(280 ft/h) or 610 m/(85 m/h)]. If the reservoir routing of the design flood indicates a change in the water surface elevation during the washout, the erosion rate would also change according to figure 30. The erosion rate should be updated during the routing to accurately predict the inflow/outflow relationship.

The discharge coefficient during the washout would be 2.75 $ft^{1/2}/s$ (1.51 $m^{1/2}/s$) (table 2). After the washout is complete the flow would be:

$$Q = CLH^{3/2} = (2.62)\ 2000\ (15.5)^{3/2}$$

$$Q = 317{,}800 \text{ ft}^3/\text{s } (9000 \text{ m}^3/\text{s})$$

BIBLIOGRAPHY

[1] Tinney, E. R., H.Y. Hsu, "Mechanics of Washout of an Erodible Fuse Plug," *Journal of the Hydraulic Division,* Proceedings, American Society of Civil Engineers, vol. 87, No. HY 3, May 1961.

[2] "Oxbow Hydroelectric Development, Idaho Spillway With Fuse Plug Control, Model Studies of Fuse Plug Washout," R. L. Albrook Hydraulic Laboratory and International Engineering Company, Inc., Washington State College, Pullman, WA, August 1959.

[3] Hsu, H.Y., "Design of Fuse Plug Spillway," *Indian Journal of Power and River Valley Development,* Hydraulic Structures Special Number, vol. 91-2, pp. 308-311 and 335, 1962.

[4] Chee, S. P., "Mobile Controls for Water Resources Projects," American Water Resources, Water Bulletin, paper No. 77072, February 1978.

[5] Morris, H. M., "Applied Hydraulic in Engineering," the Ronald Press Co., New York, NY, 1963.

[6] Vanoni, Vito A., "Sedimentation Engineering," American Society of Civil Engineers, ASCE Task Committee for Preparation of the Manual on Sedimentation of the Sedimentation Committee of the Hydraulics Division, No. 54, New York, NY, 1975.

[7] Rouse, H., "Elementary Mechanics of Fluids," John Wiley & Sons, Inc., London, pp. 201-203, October 1948.

BEST COPY AVAILABLE

[8] Kamphius, J. W., "Determination of Sand Roughness for Fixed Beds," *Journal of Hydraulic Research* 12 (1974) No. 2.

[9] Bos, M. G., "Discharge Measurement Structures," Publication No. 20, International Institute for Land Reclamation Improvement, Wageningen, The Netherlands.

[10] King, H. W., "Handbook of Hydraulics," McGraw Hill Book Co., New York, NY, 1963.

Pugh, C. A., and E. W. Gray, Jr., "Fuse Plug Embankment in Auxiliary Spillways — Developing Design Guidelines and Parameters," In: *Dam Safety and Rehabilitation, Fourth Annual USCOLD Lecture*, Bureau of Reclamation, Denver, CO, January 1984.

BEST COPY AVAILABLE

BLANK PAGE

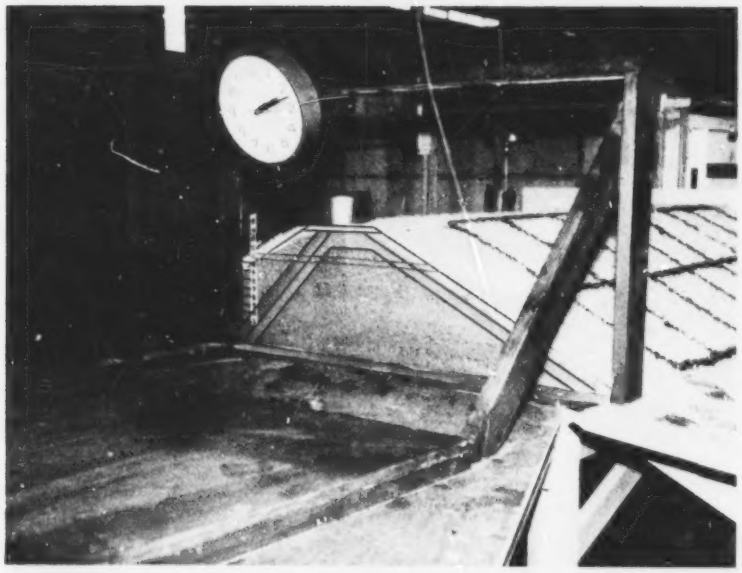

Figure 1. -- Model fuse plug embankment, test No. 7. P801-D80944.

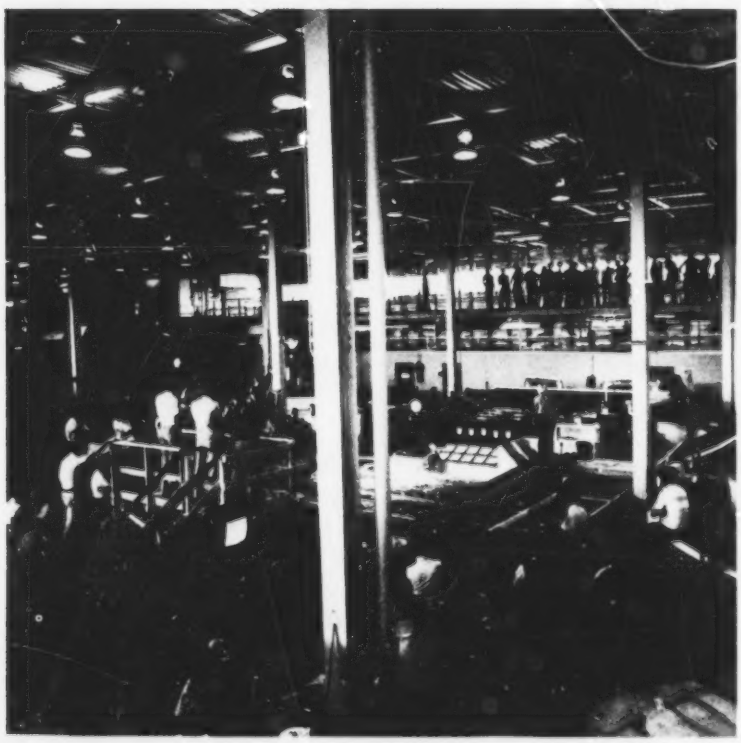

Figure 2. – Model operation, test No. 4. P801-D80945.

BEST COPY AVAILABLE

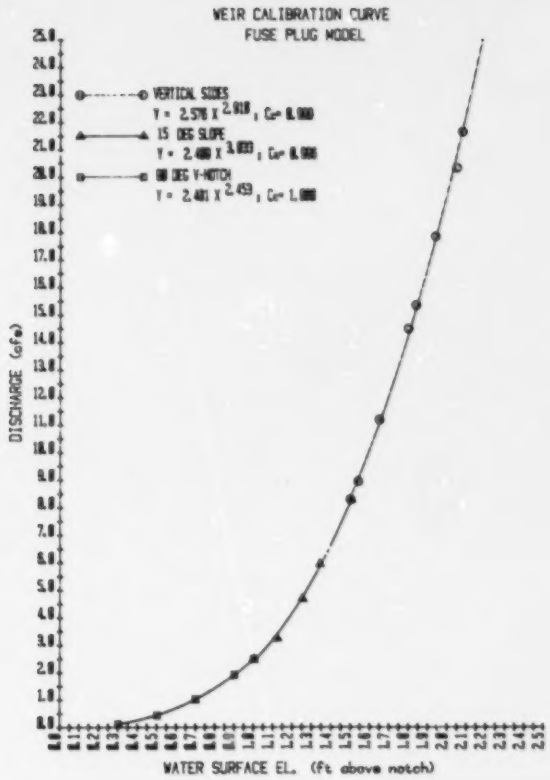

Figure 3. – Flow measurement weir calibration curve (1 ft = 0.3048 m, 1 ft^3/s = 0.02832 m^3/s).

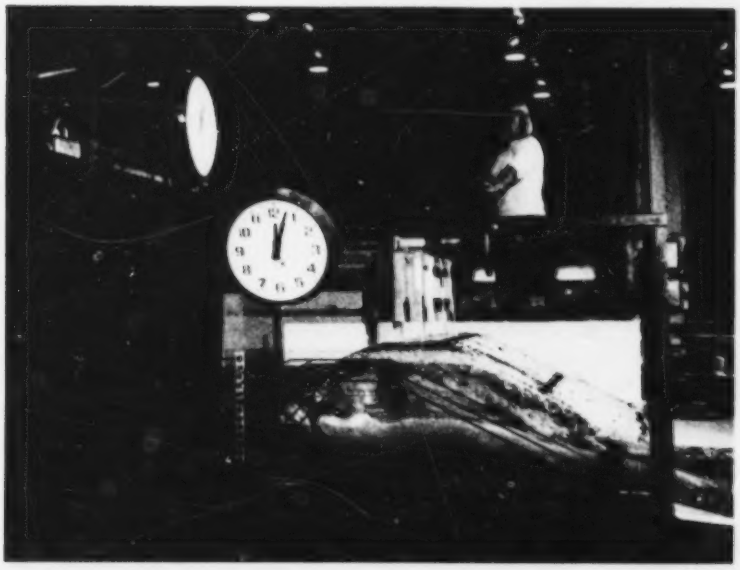

Figure 4. – Initial breach viewed through end wall, test No. 8. P801-D80946.

BEST COPY AVAILABLE

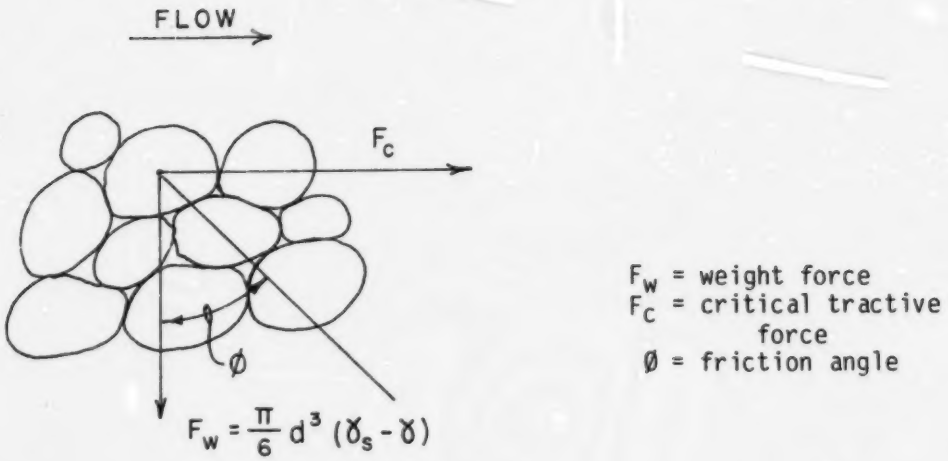

Figure 5. – Forces on a sediment particle.

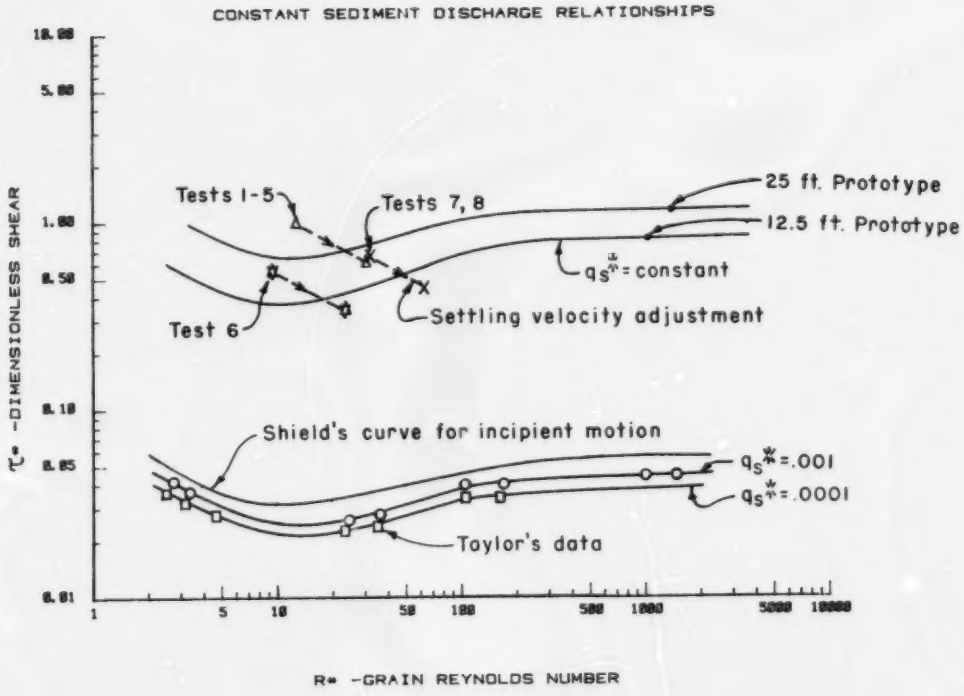

Figure 6. – Dimensionless unit sediment discharge curves versus dimensionless shear and grain Reynolds number.

BEST COPY AVAILABLE

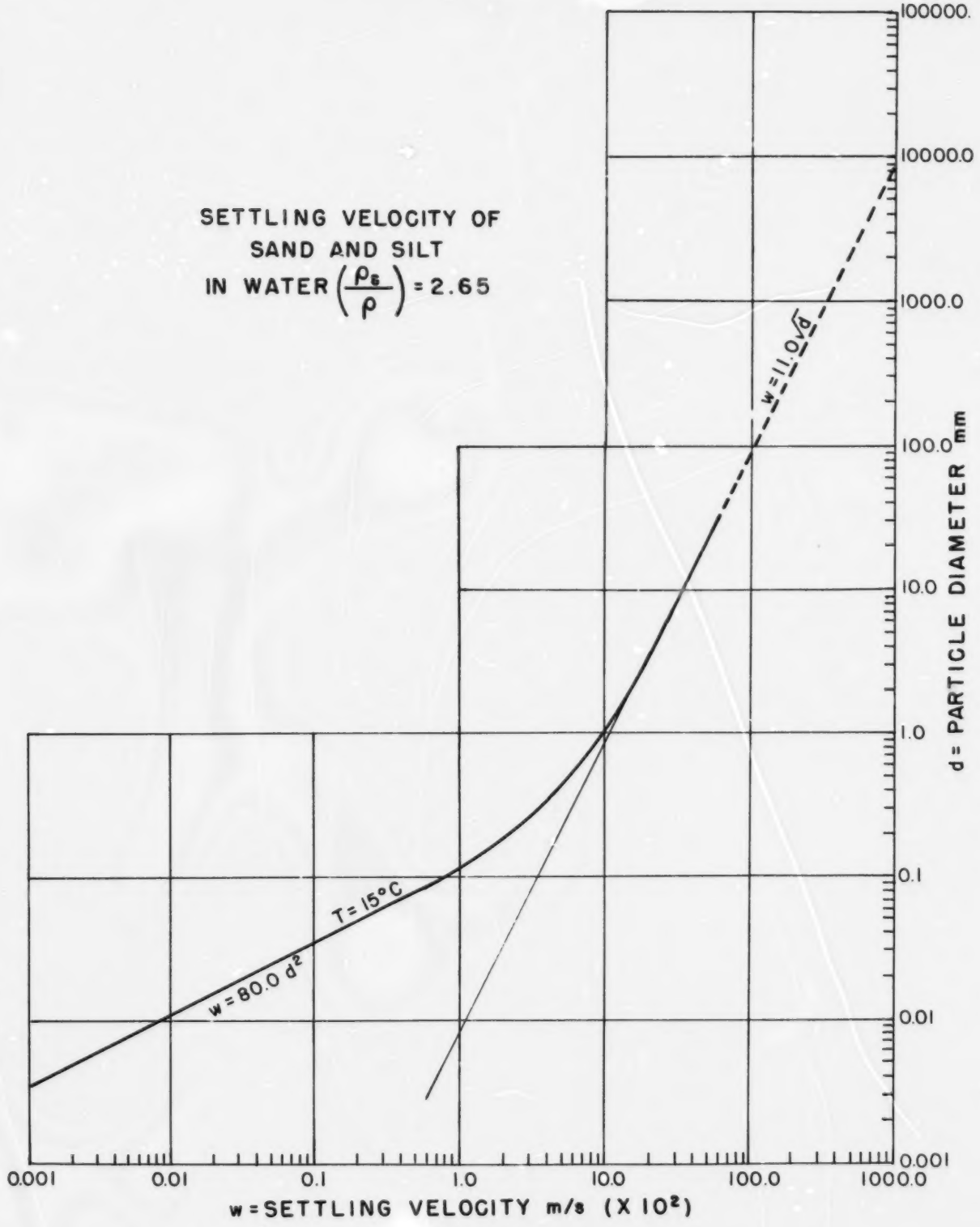

Figure 7. – Settling velocity of sand and silt in water (1 ft = 0.3048 m).

BEST COPY AVAILABLE

(1) CORE MATERIAL

(2) SAND FILTER

(3) COMPACTED SAND AND GRAVEL

(4) SLOPE PROTECTION

(5) GRAVEL SURFACING

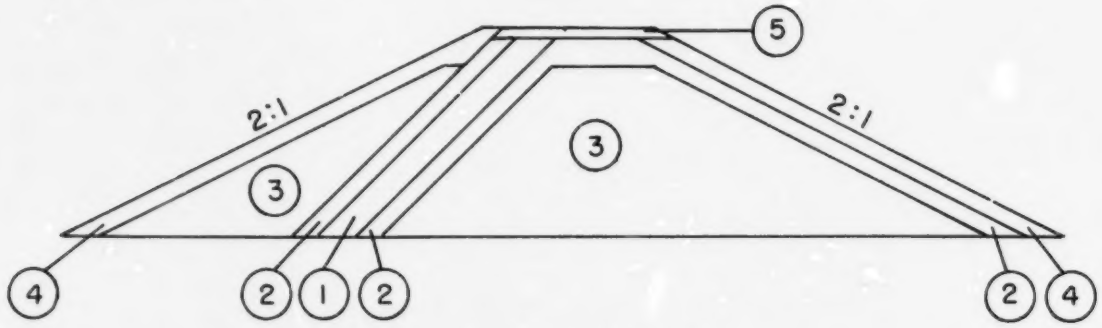

EMBANKMENT

(6) COMPACTED ROCKFILL

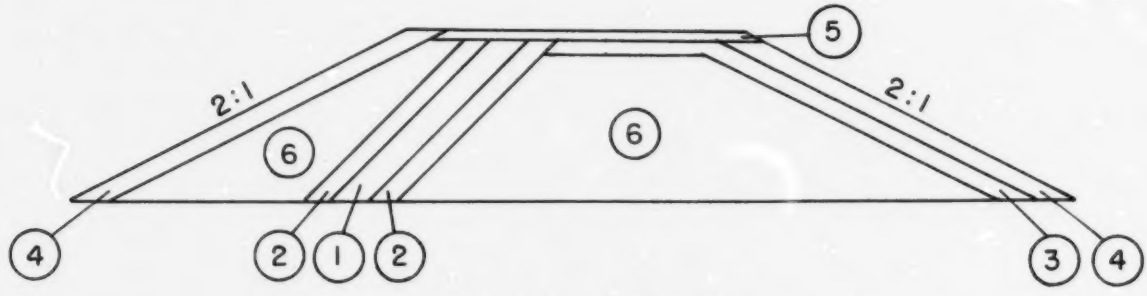

PILOT CHANNEL

Figure 8. – Fuse plug embankment and pilot channel cross sections.

BEST COPY AVAILABLE

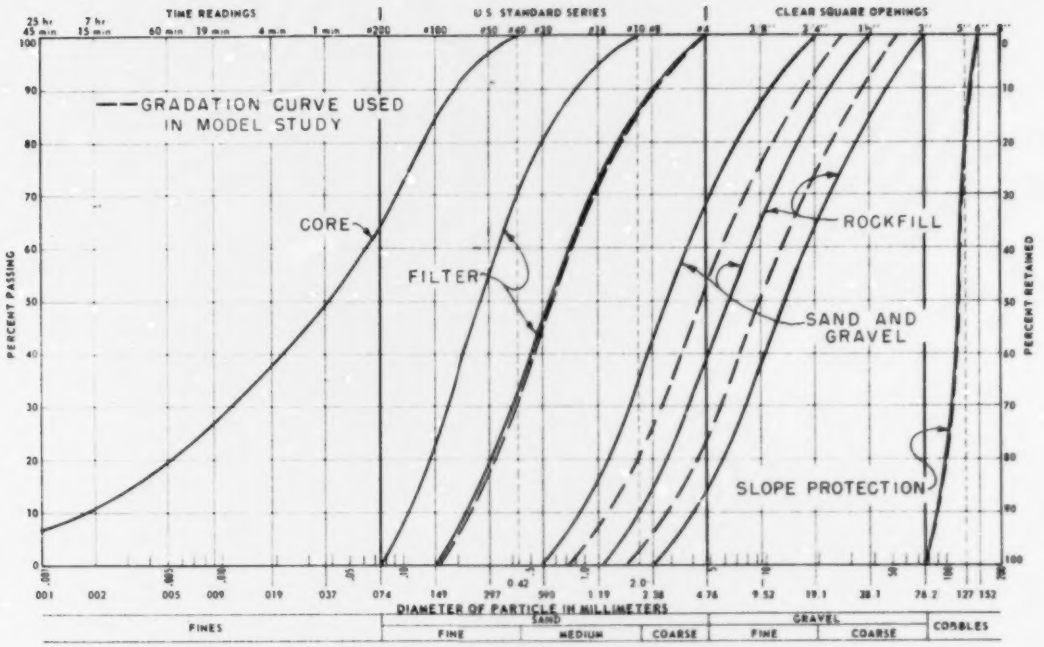

Figure 9. – Prototype gradation curves.

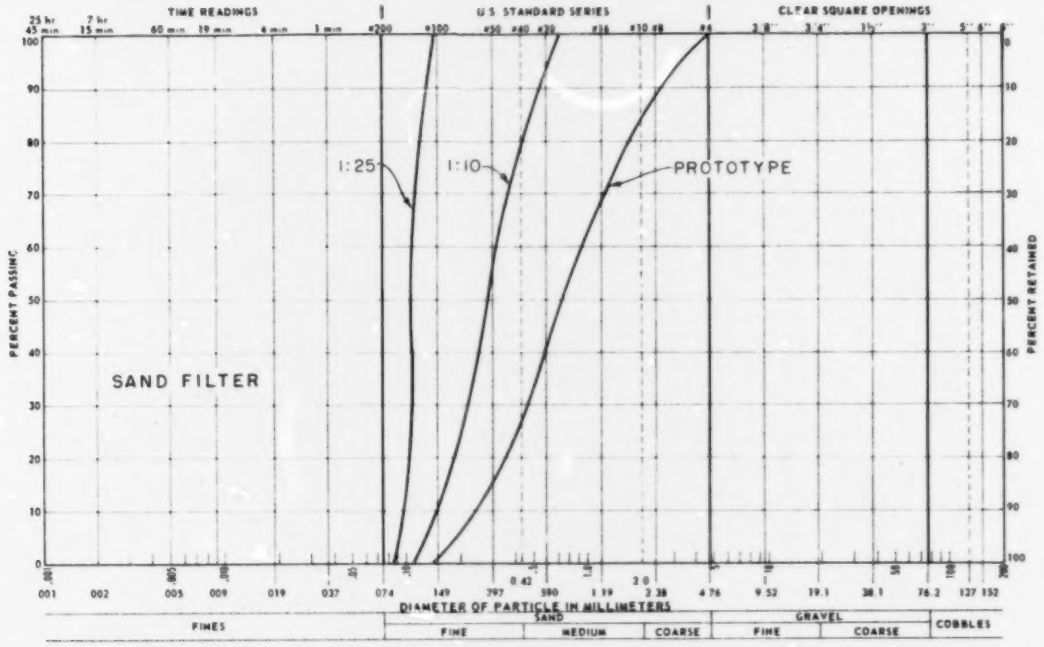

Figure 10. – Gradation curves, sand filter.

BEST COPY AVAILABLE

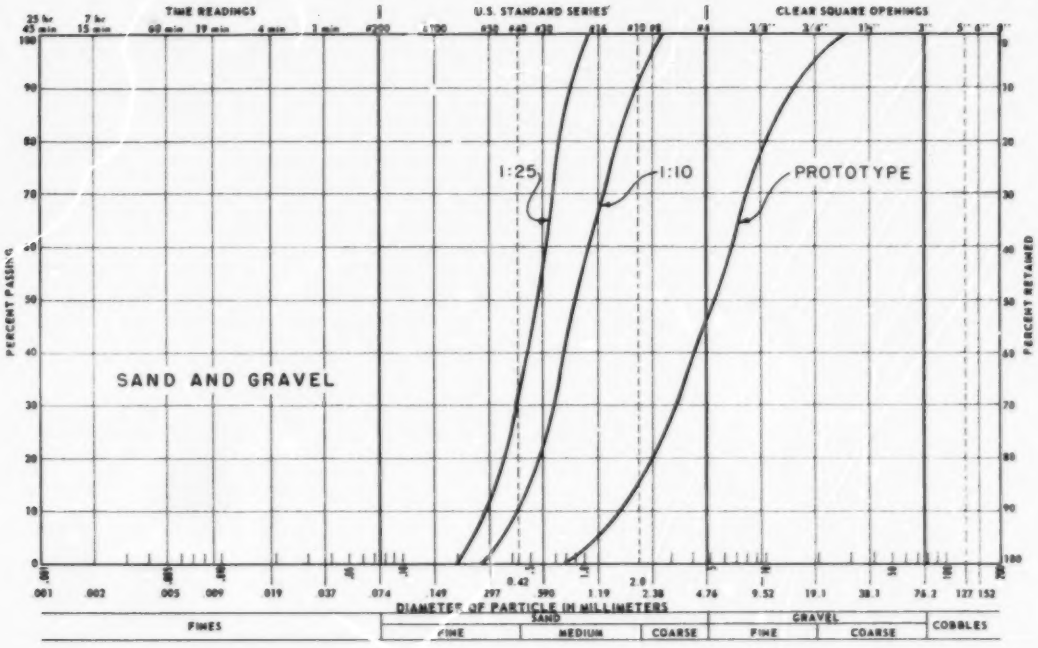

Figure 11. – Gradation curves, sand and gravel.

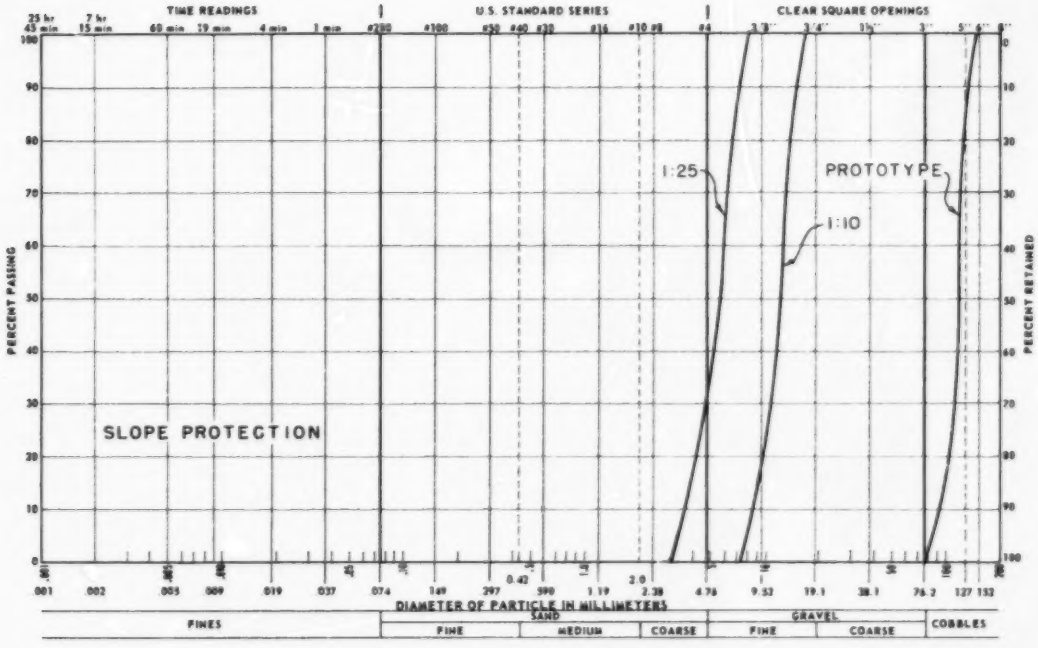

Figure 12. – Gradation curves, slope protection.

BEST COPY AVAILABLE

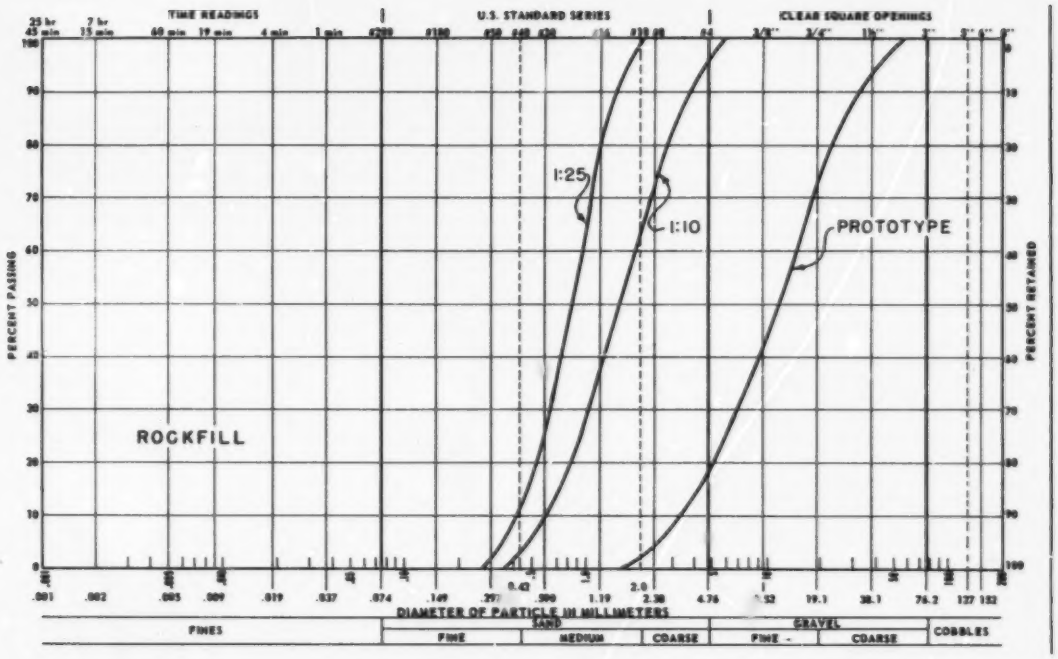

Figure 13. – Gradation curves, rockfill.

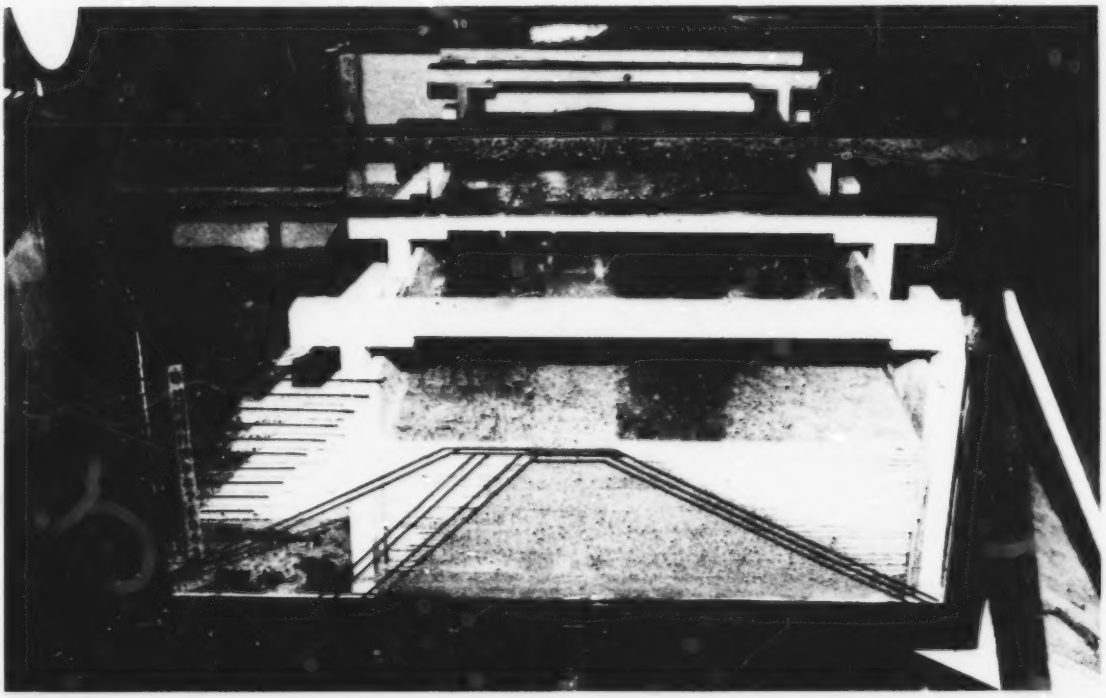

Figure 14. – Model fuse plug embankment placement. P801-D80947.

BEST COPY AVAILABLE

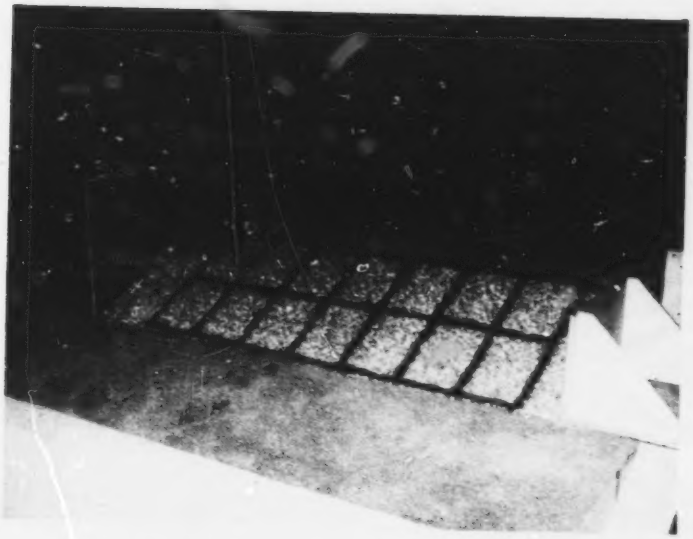

Figure 15. – Model fuse plug embankment. P801-D80945.

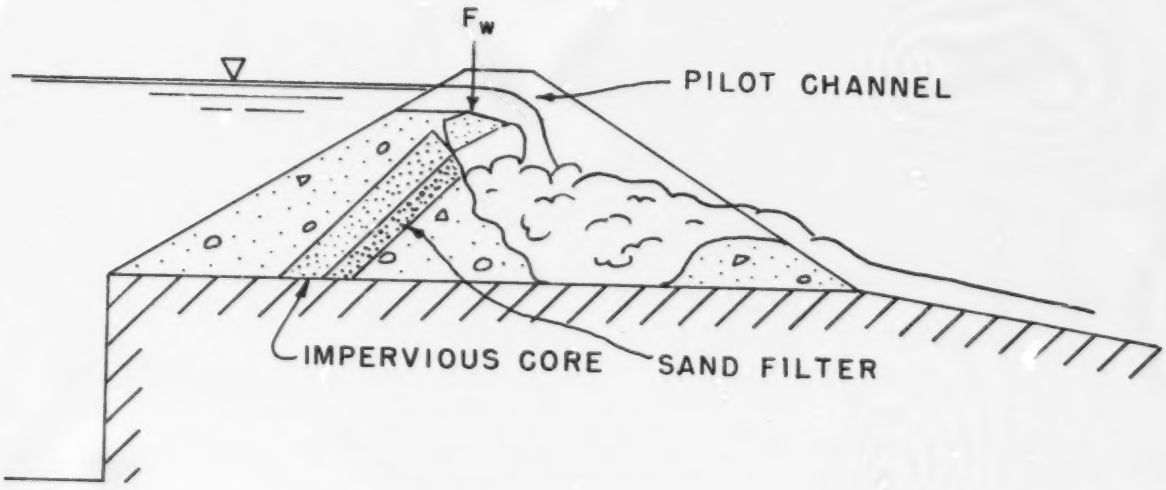

Figure 16. – Flow through the pilot channel showing the failure mode of the impervious core.

BEST COPY AVAILABLE

Test No.	*H*, ft	Scale	*W/H*	*B/H*	*b/H*	θ deg	*T/H*	*t/H*	*L/H*	*p/H*	*h/H*	Sand filter	*D/J*	*D/H*	*ER*, ft/min
1	1.0	1:25	0.4	4.4	3.1	45	0.12	0.04	0.0	0.24	0.12	Yes	0.21	0.92	1.74
2	1.0	1:25	.4	4.4	3.1	45	.12	.12	.12	.36	.12	No	.21	.92	1.52
3	1.0	1:25	.4	4.4	4.0	30	.12	.04	.32	.48	.12	No	.21	.92	1.53
4	1.0	1:25	.4	4.4	3.1	45	.12	.04	3.24	.48	.12	No	.21	.92	1.55
5	1.0	1:25	.8	4.8	3.4	45	.12	.04	0.45	.74	.12	Yes	.15	.92	1.60
6	0.5	1:25	.8	4.8	3.4	45	.12	.04	.91	1.48	.24	Yes	.07	.84	0.68
7	1.25	1:10	.8	4.8	3.4	45	.12	.04	.51	0.88	.24	Yes	.17	.84	1.66
													*.15	*.73	*1.43
8	1.25	1:10	.8	4.8	3.4	45	.12	.04	1.60	3.20	.24	Yes	*.12	*.60	*0.63

1 ft = 0.3048 m
* The upstream water level (*D*) was lowered.

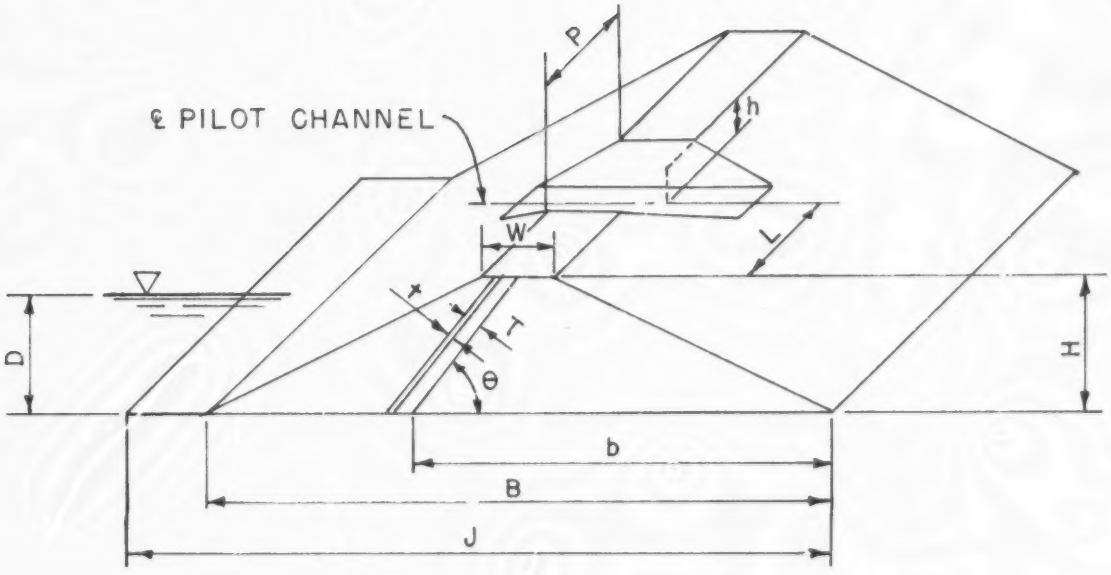

Figure 17. – Definition sketch of geometric features of model fuse plug embankment.

BEST COPY AVAILABLE

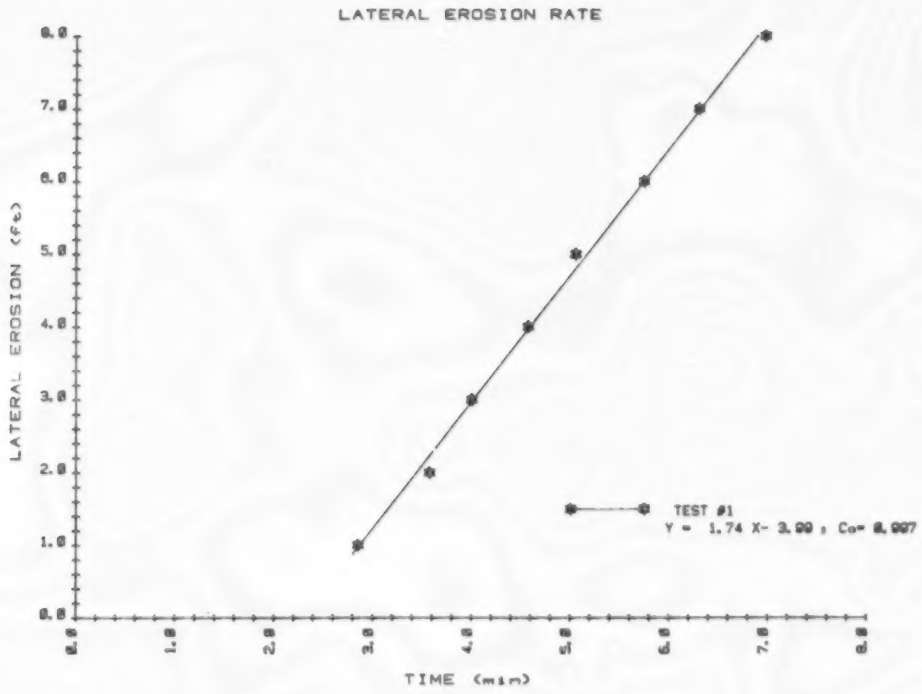

Figure 18. – Lateral erosion rate, test No. 1.

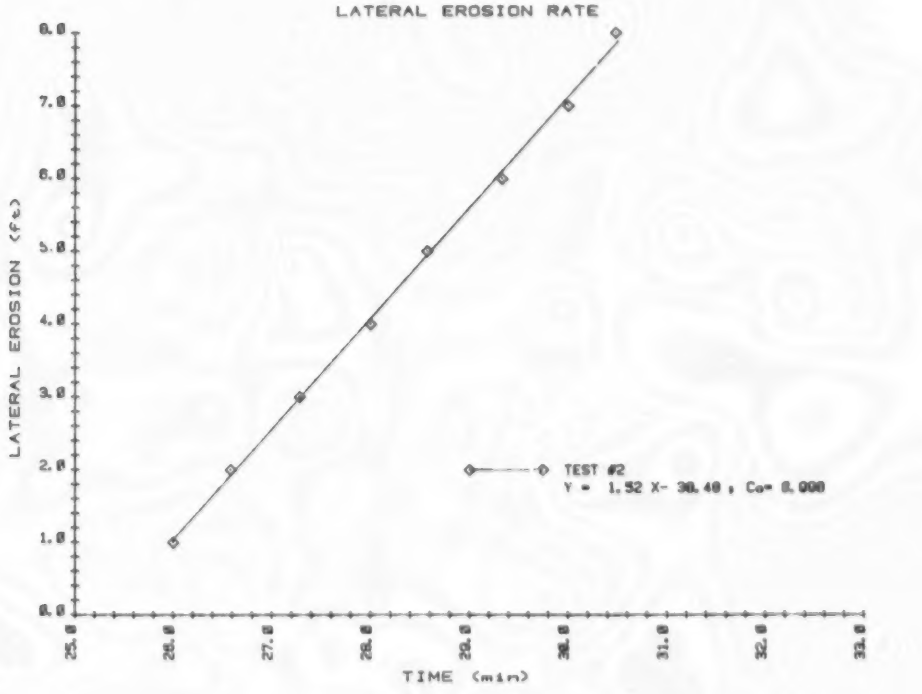

Figure 19. – Lateral erosion rate, test No. 2.

BEST COPY AVAILABLE

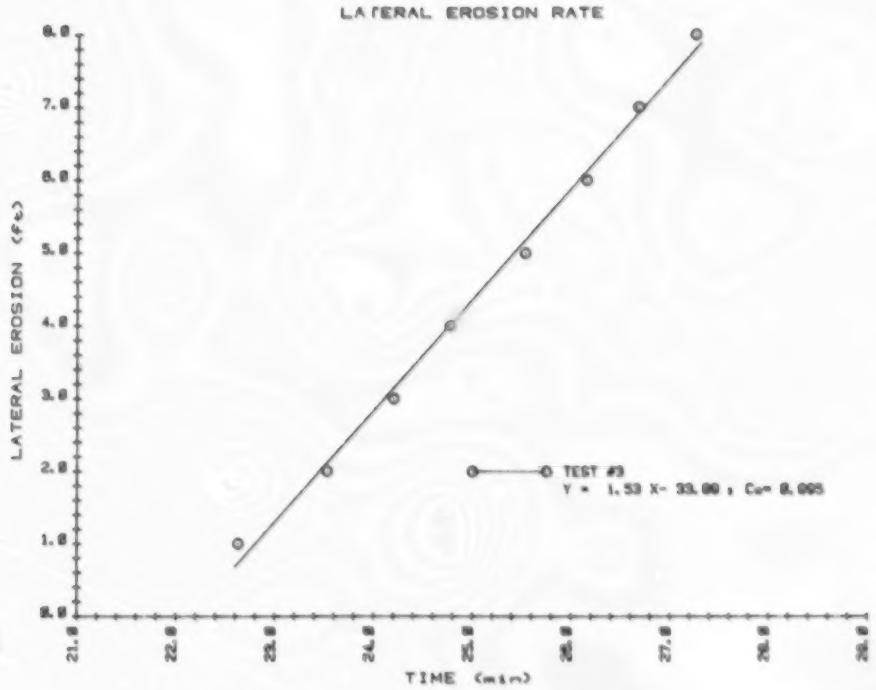

Figure 20. – Lateral erosion rate, test No. 3.

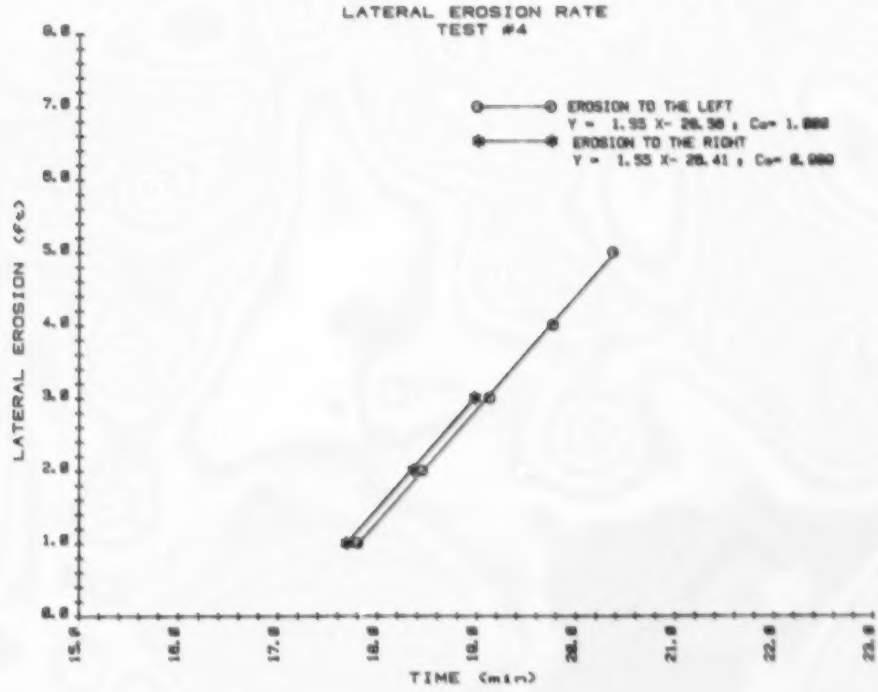
LATERAL EROSION RATE
TEST #4
LATERAL EROSION (ft)
TIME (min)
EROSION TO THE LEFT
Y = 1.55 X- 28.58 ; Cc= 1.000
EROSION TO THE RIGHT
Y = 1.55 X- 28.41 ; Cc= 0.999

Figure 21. – Lateral erosion rate, test No. 4.

BEST COPY AVAILABLE

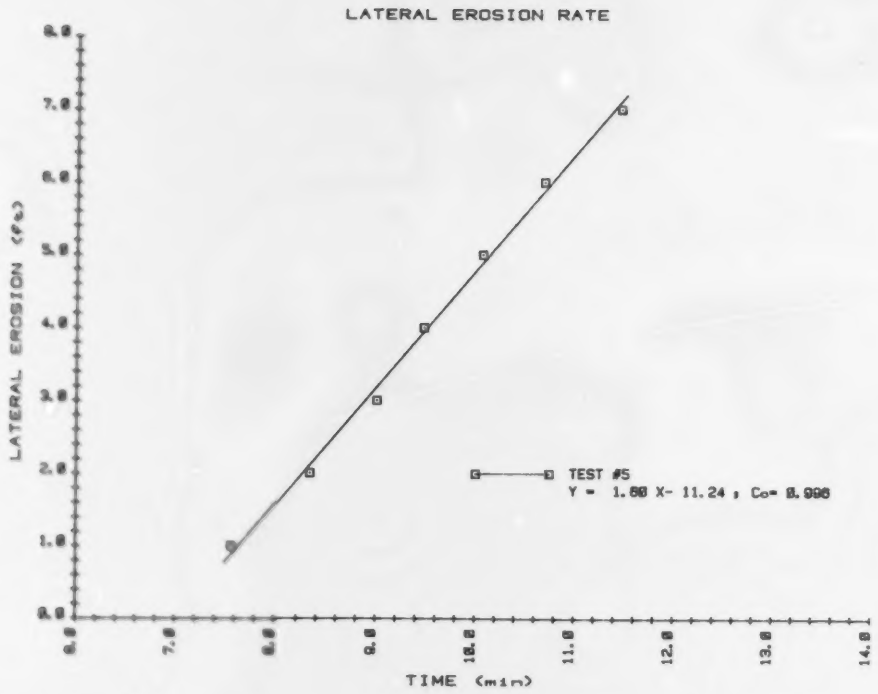

Figure 22. – Lateral erosion rate, test No. 5.

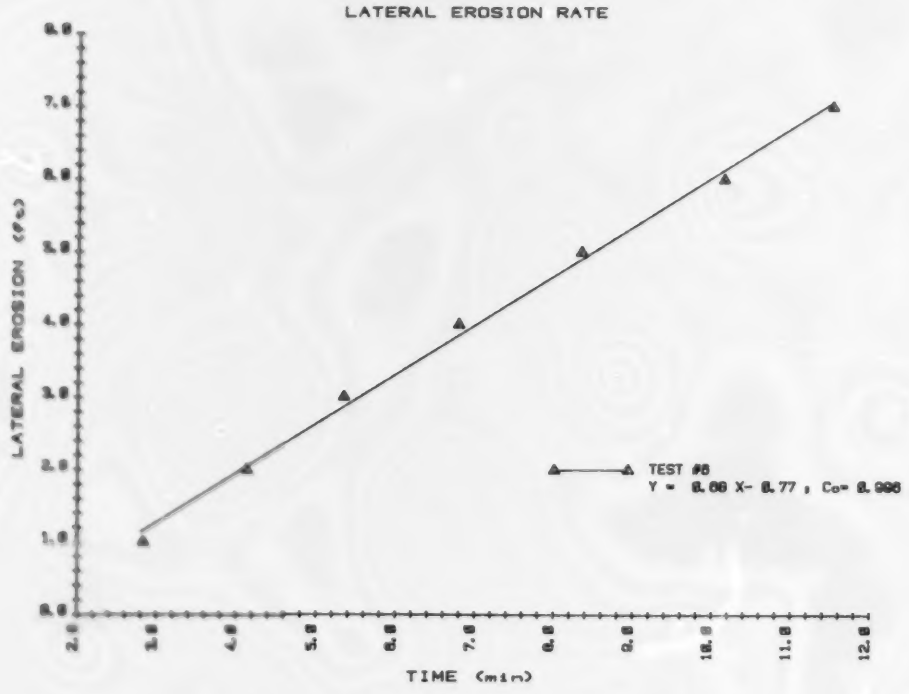

Figure 23. – Lateral erosion rate, test No. 6.

BEST COPY AVAILABLE

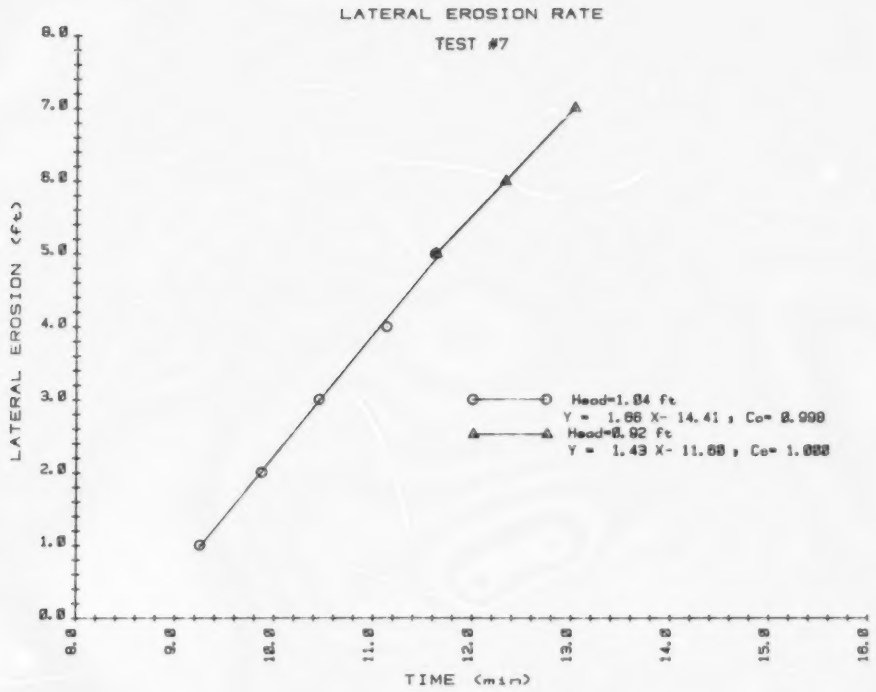

Figure 24. – Lateral erosion rate, test No. 7.

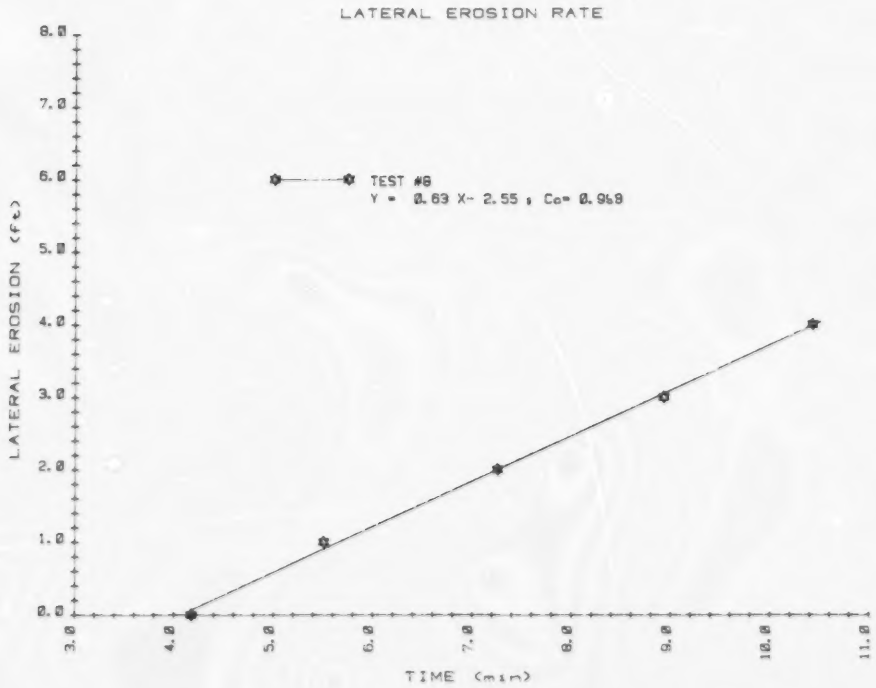

Figure 25. – Lateral erosion rate, test No. 8.

BEST COPY AVAILABLE

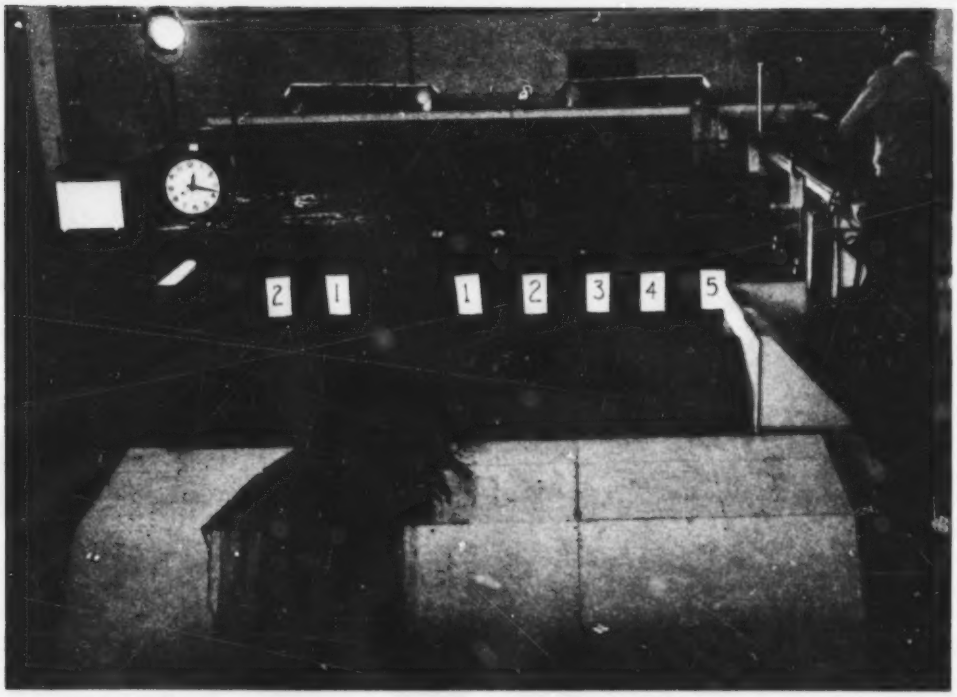

(a) Water flowing through the pilot channel over the clay core. P801-D80949.

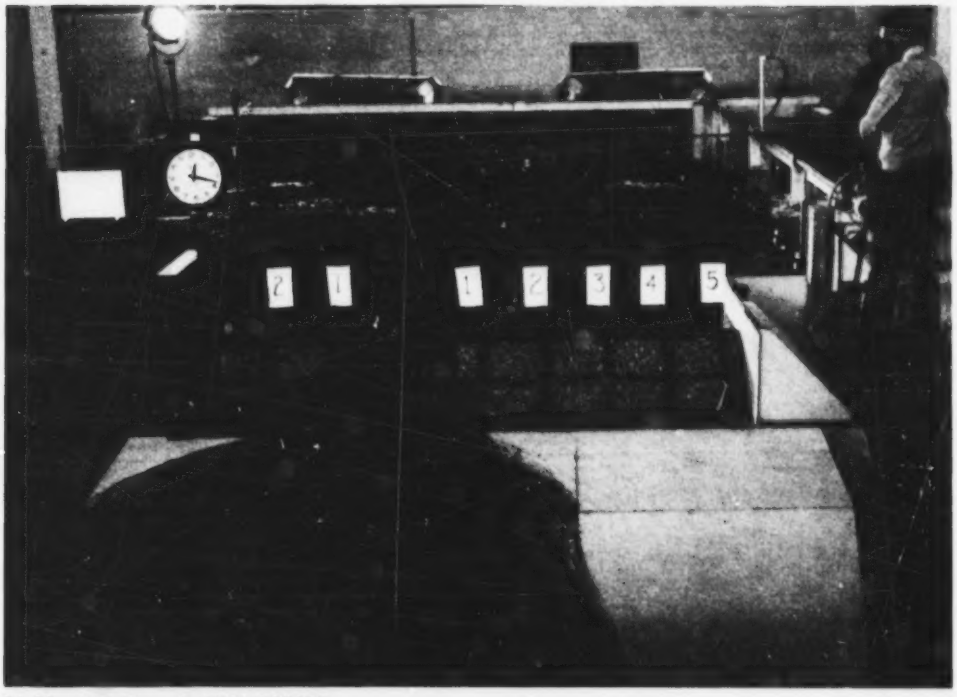

(b) After initial breach. P801-D80950.

Figure 26. – Views of the washout process.

BEST COPY AVAILABLE

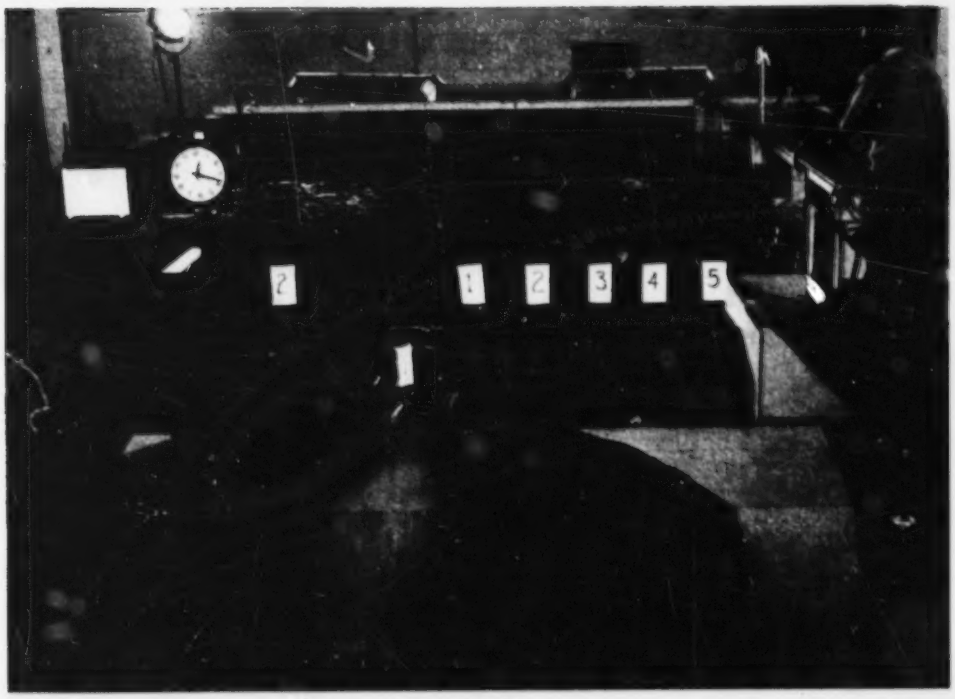

(c) The lateral erosion process is underway. P801-D80951.

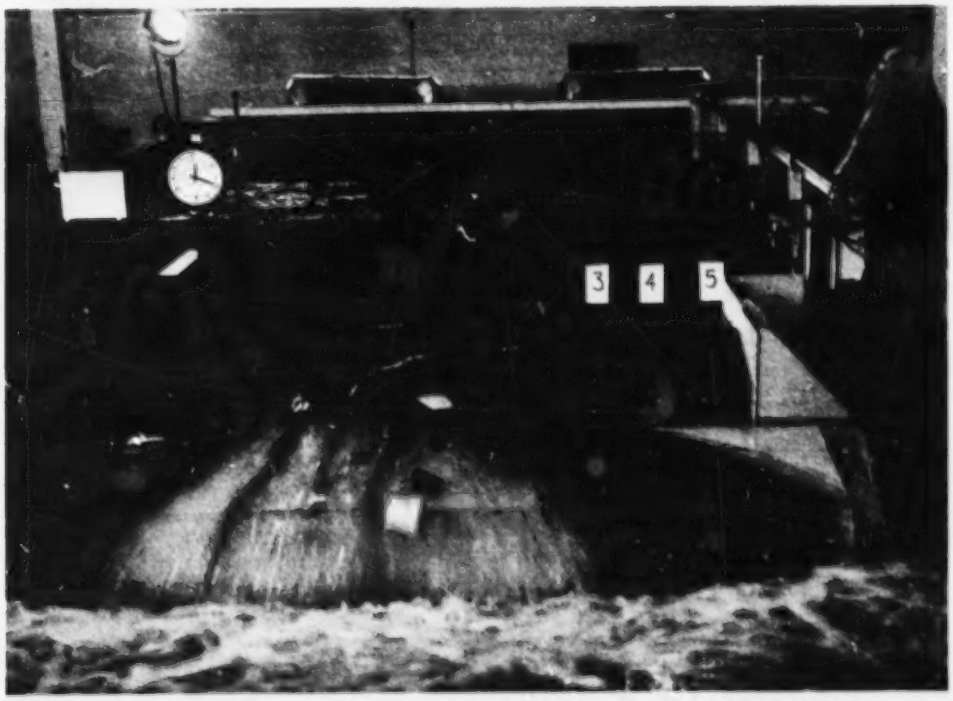

(d) The lateral erosion rate was determined by timing the erosion between flags. P801-D80952.

Figure 26. – Views of the washout process. – Continued

BEST COPY AVAILABLE

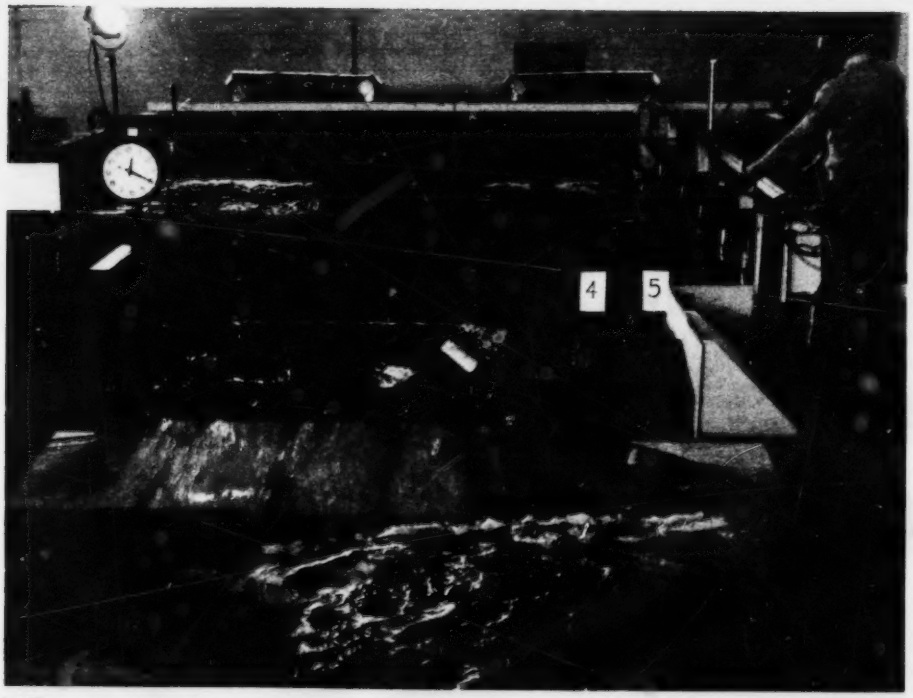

(e) The reservoir elevation was held constant by the long adjustable weir in the background. P801-D80953.

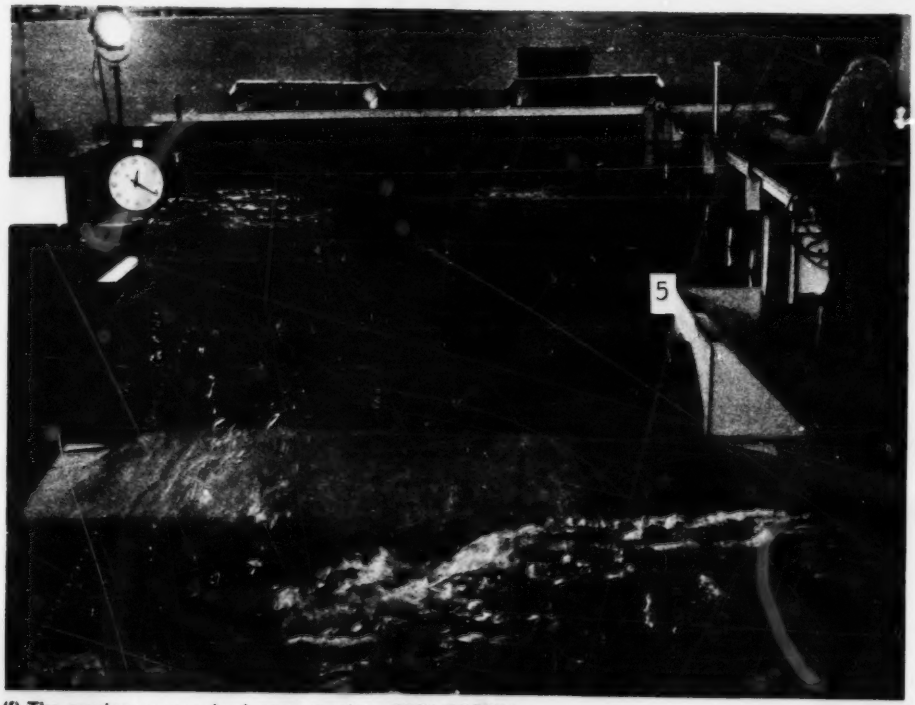

(f) The erosion process is almost complete. P801-D80954.

Figure 26. – Views of the washout process. – Continued

BEST COPY AVAILABLE

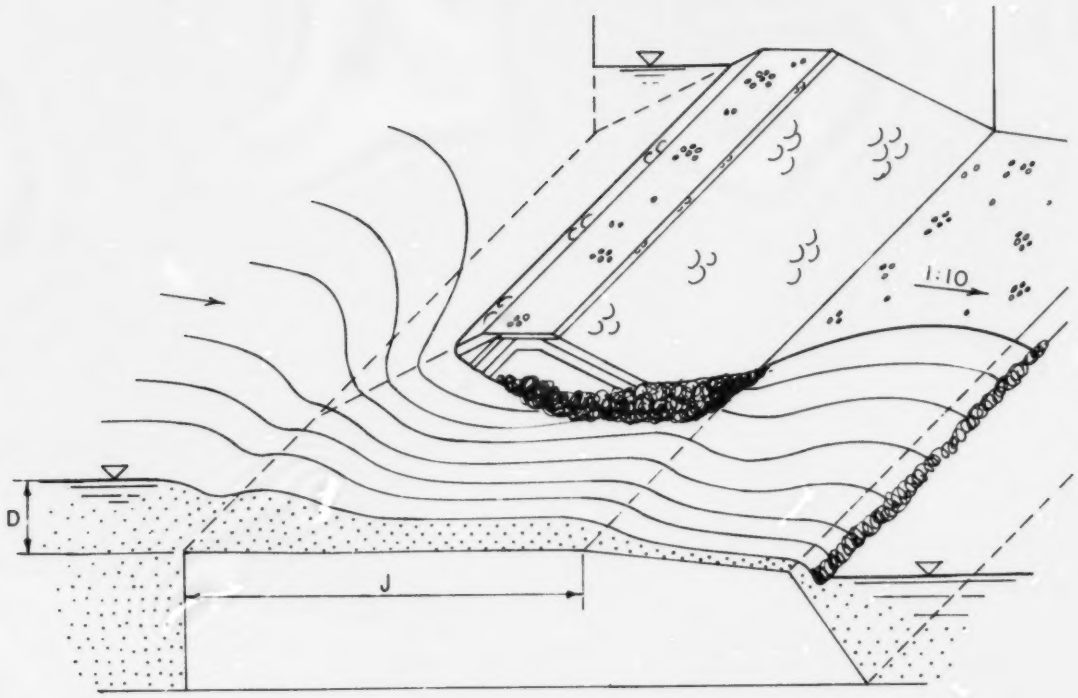

Figure 27. – Schematic of the lateral erosion process. The water flows across the face of the embankment, around the core, and erodes the noncohesive material downstream from the core.

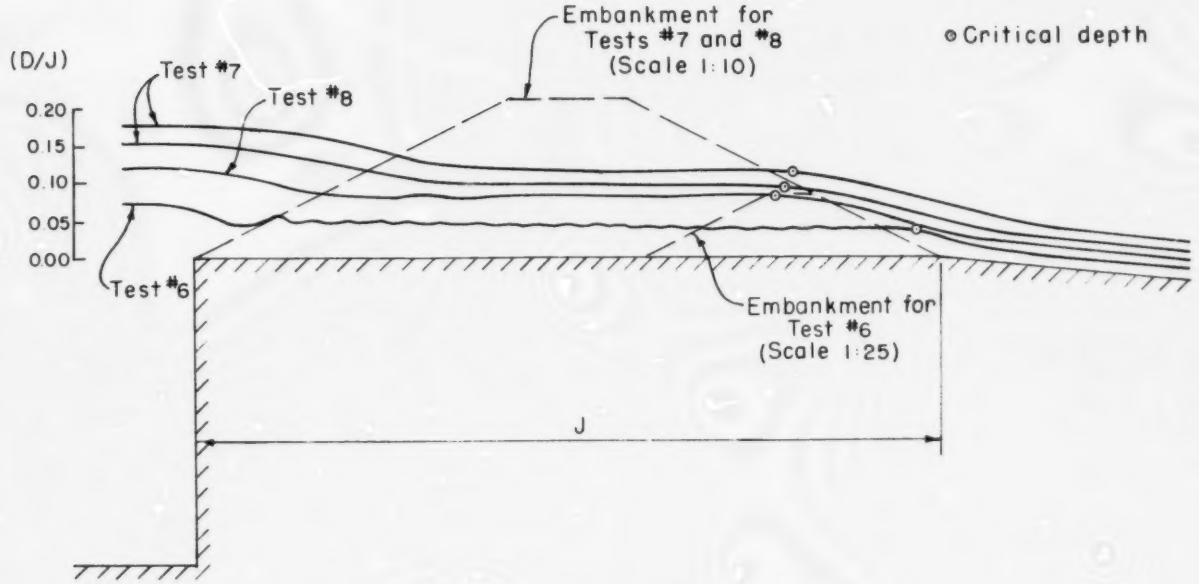

Figure 28. – Broad-crested weir flow profiles, tests No. 6, 7, and 8.

BEST COPY AVAILABLE

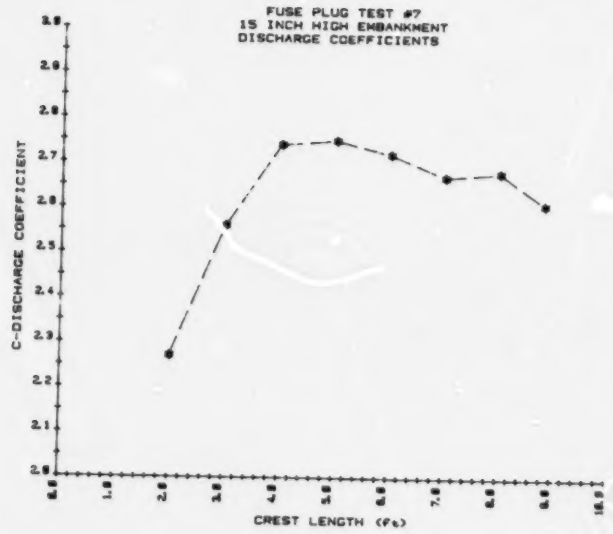

Figure 29. – Weir formula discharge coefficients, test No. 7.

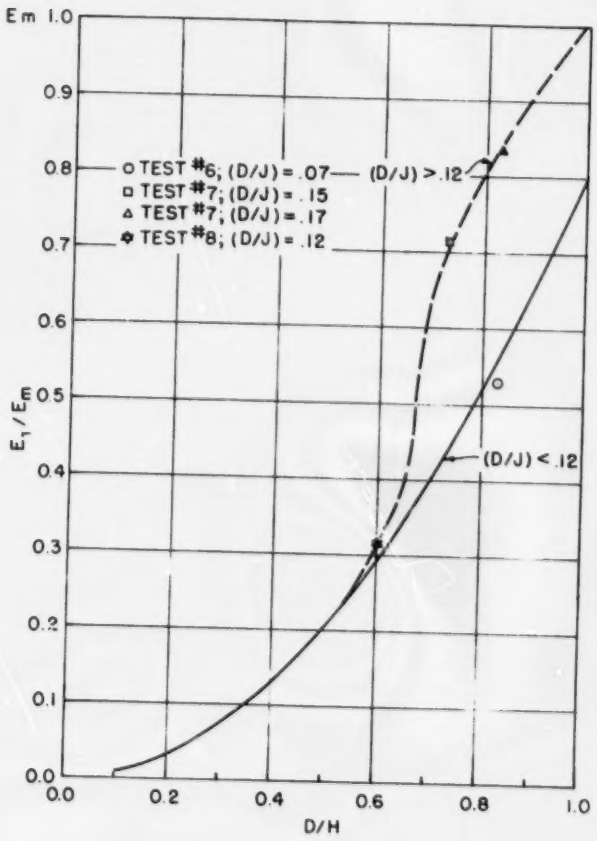

Figure 30. – Relative erosion rates after breach, used to adjust computed erosion rates (see fig. 31) for varying water depths and crest lengths (data values adjusted to the same scale).

BEST COPY AVAILABLE

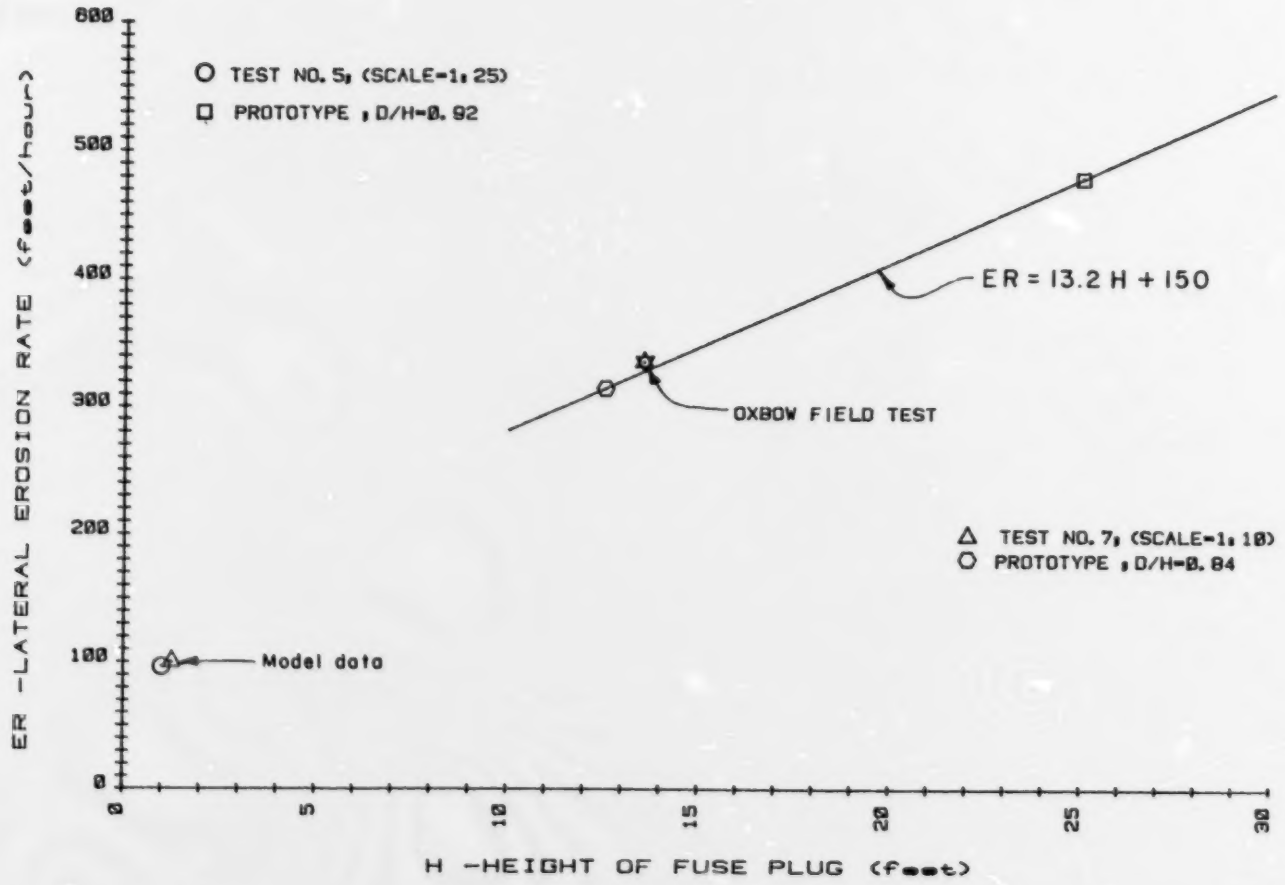

Figure 31. – Lateral erosion rates (after initial breach) for a fuse plug embankment with the geometric features of tests No. 5 and 7 (see table 1).

BEST COPY AVAILABLE

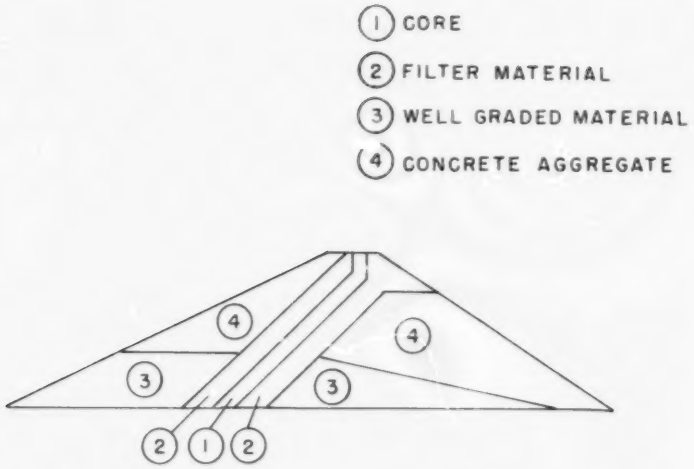

Figure 32. – Embankment design for Oxbow field test.

GPO 850-139

BEST COPY AVAILABLE

Mission of the Bureau of Reclamation

The Bureau of Reclamation of the U.S. Department of the Interior is responsible for the development and conservation of the Nation's water resources in the Western United States.

The Bureau's original purpose "to provide for the reclamation of arid and semiarid lands in the West" today covers a wide range of interrelated functions. These include providing municipal and industrial water supplies; hydroelectric power generation; irrigation water for agriculture; water quality improvement; flood control; river navigation; river regulation and control; fish and wildlife enhancement; outdoor recreation; and research on water-related design, construction, materials, atmospheric management, and wind and solar power.

Bureau programs most frequently are the result of close cooperation with the U.S. Congress, other Federal agencies, States, local governments, academic institutions, water-user organizations, and other concerned groups.

A free pamphlet is available from the Bureau entitled "Publications for Sale." It describes some of the technical publications currently available, their cost, and how to order them. The pamphlet can be obtained upon request from the Bureau of Reclamation, Attn D-822A, P O Box 25007, Denver Federal Center, Denver CO 80225-0007.

BEST COPY AVAILABLE